Summer 2007

Adhesion-delamination mechanics of linear and axisymmetric film at film-substrate interface

Ming-Fung Wong

Department:

ADHESION-DELAMINATION MECHANICS OF LINEAR AND AXISYMMETRIC FILM AT FILM-SUBSTRATE INTERFACE

by

MING-FUNG WONG

A THESIS

Presented to the Faculty of the Graduate School of the

UNIVERSITY OF MISSOURI-ROLLA

In Partial Fulfillment of the Requirements for the Degree

MASTER OF SCIENCE IN MECHANICAL ENGINEERING

2007

Approved by

Kai Tak Wan, Advisor

Brad Miller

Chang-Soo Kim

ABSTRACT

This thesis is to characterize the thin membrane adhesion-delamination phenomena which occur in biological cells and micro-electro-mechanical systems (MEMS) operation. The delamination of a thin film adhered to a rigid substrate is subjected to the coupling effects of tensile residual stress and interfacial adhesion energy. The adhesion-delamination mechanics is derived using the classical linear elasticity and thermodynamics energy balance. The membrane deformation is here dominated by a mixed plate-bending and membrane-stretching, while the concomitant stress is neglected. An 1-dimensional model is first investigated where a pre-stressed rectangular film clamped at both ends delaminates from a rigid punch of the same dimension as the film width. Upon a tensile external load applied to the rigid punch, “Pinch-off”, or stable shrinking of the contact area to a line prior to complete detachment, is predicted. The 1-dimensional model is further extended to a 2-dimensional axisymmetric geometry. A thin circular film clamped at the periphery detaches from the planar surface of a rigid cylindrical punch upon external load. “Pull-off”, or spontaneous detachment from the substrate, occurs when the contact circle shrinks to between 0.1758 and 0.3651 times the film radius depending on the magnitude of the residual membrane stress. The finite “pull-off” radius differs from the 1-dimensional counterpart. The models are useful in understanding the behavior of various adhesion-delamination phenomena, such as capacitive MEMS-RF switches, micro pumps, microstructure network, and nanostructures.

ACKNOWLEDGMENTS

I am thankful to my advisor Dr. Kai-tak Wan for guiding me throughout this research, and he has given me opportunities to present part of the results at various conferences. The present thesis is a continuation of my earlier work sponsored by the Opportunity for Undergraduate Research Experiences (OURE) program at the University of Missouri-Rolla which was also supervised by Dr. Wan. I greatly appreciate the sponsorship from the University of Missouri Research Board (# 2428) and the US National Science Foundation (NSF# CMS-0527912), which has made my research possible.

I am grateful to my parents, Mr. Wing-fai Wong and Mrs. Chung-siu Lau, for their unfailing love, caring, encouragements and support. It is impossible for me even to comprehend completing my bachelor's and master's degrees at University of Missouri-Rolla without them.

TABLE OF CONTENTS

LIST OF ILLUSTRATIONS

LIST OF TABLES

NOMENCLATURE

Symbol	Description
x	Directional Coordinate used in the 1-D Rectangular Model
r	Directional Coordinate used in the 2-D Axisymmetric Model
l	Half of the Length of the Film Model in the 1-D Rectangular model
a	Radius of Film in the 2-D Axisymmetric Model
c	Half of the Contact Length between Two Contact Objects in 1-D Rectangular Model and the Contact Radius in 2-D Axisymmetric Model
h	Film Thickness
w	Profile of Film
w_0	Central Displacement of Film
γ	Adhesion Energy/Surface Energy Density (Energy/Area)
σ	Membrane Stress
σ_0	Residual Membrane Stress
F	External Force
U_T	Total Energy of the Punch-Film System
U_P	Potential Energy of the Punch-Film System
U_E	Elastic Energy Stored in Deformed Membrane
U_S	Surface Energy at Contact Area among Two Contact Subjects
∇^2	Laplacian Operator in Either Rectangular or Cylindrical Coordinate System
ξ	r/a or x/l
λ	c/l
ζ	c/a
ω	w/h
ω_0	w_0/h
φ	$\frac{l^3}{2\kappa h}F$ or $\frac{Fa^2}{2\pi\kappa h}$

Symbol	Description
Γ	$\left(\frac{l^4}{\kappa h^2}\right)\gamma$ or $\left(\frac{a^4}{2\kappa h^2}\right)\gamma$
β	$\left(\frac{l^2 h}{\kappa}\right)^{1/2}\sigma_0^{1/2}$ or $\left(\frac{a^2 h}{\kappa}\right)^{1/2}\sigma_0^{1/2}$
Σ_T	$\frac{l^3}{2\kappa h^2}U_T$ or $\frac{a^2}{2\pi\kappa h^2}U_T$
Σ_P	$\frac{l^3}{2\kappa h^2}U_P$ or $\frac{a^2}{2\pi\kappa h^2}U_P$
Σ_E	$\frac{l^3}{2\kappa h^2}U_E$ or $\frac{a^2}{2\pi\kappa h^2}U_E$
Σ_S	$\frac{l^3}{2\kappa h^2}U_S$ or $\frac{a^2}{2\pi\kappa h^2}U_S$
n	Slope of the Constitutive Relation Delamination Trajectory

1. INTRODUCTION

1.1. THIN FILM ADHESION-DELAMINATION IN BIOLOGICAL STUDY

In biology, individual cells adhere and move from one location to another via non-specific (e.g. electrostatic) and specific (e.g. ligand-receptor interactions) adhesion to form multi-cell aggregates (Figures 1.1 [1] and 1.2[2]), 2-D and 3-D tissues [2]. Because most cells are thin-walled capsules with an ultra-thin lipid bilayer membrane down to 100 Å in thickness, interactions between cells are achieved by thin film adhesion. Situations exist when biochemical processes, such as osmosis [3, 4] and shear due to fluid flow [5, 6], generate mechanical stresses in the cell membranes that are capable of detaching a cell from an adhering substrate. Interfacial adhesion-delamination also provides the key to cell locomotion [2].

Figure 1.1. Multi-Cell Aggregates

Figure 1.2. Cell Locomotion Along a Flat Substrate

1.2. THIN FILM ADHESION-DELAMINATION IN ELECTRONIC DEVICES

Physics between surfaces and components down to the microscopic scale is different from what usually transpires in the macroscopic scale. Electrostatics due to stray charges, meniscus formation due to water condensation, van der Waals interactions, and DLVO (Derjaguin, Landau, Verwey and Overbeek) [7] double layers play significant roles in microscopic scale electronics and interface of movable components. Many concepts of conventional macroscopic engineering structures and machines fail badly in the microscopic regime, for instances, electromechanical systems (MEMS) involving moveable parts [8] and stiction in microbeams and microstructures [9-11], as well as nanomachines in the molecular dimension [8, 10]. When an electrostatic potential in a typical MEMS-RF switch (Figure 1.3) is applied to the pad directly underneath the

mechanically suspended bridge, the moveable film attaches to the substrate, giving rise to an electrical signal [12, 13]. Upon removal of the potential, an ideal bridge resumes its undeformed planar geometry. In reality, however, the presence of adhesion at the film-substrate interface hinders the elastic recovery and can cause the device to fail [8]. Further complications arise if the bridge is pre-stressed as a result of thermal mismatch between the bridge, clamps, and silicon substrate during fabrication or during device operation. A better understanding of the adhesion-delamination mechanism will therefore enhance better design, optimize performance, and reliability. Another application is the stability of micro-beam networks. The presence of significant surface forces due to high relative humidity, van der Waals interactions, and stray electrostatic charges could lead to collapse of the microstructure.

Residual membrane stress can change the apparent stiffness and behavior of thin film delamination. Residual stresses that are induced in the films as a result of fabrication processes, mismatch of thermal expansion coefficients of film and substrate, and heat dissipation during device operation further complicate the already involved stiction problems. To improve the design criteria and to assess component reliability, it is vital to gain a better understanding of the device behavior due to the coupled interfacial stiction and residual stress.

“ON” Stage “OFF” Stage

Figure 1.3. Typical MEMS-RF-Switch Design

1.3. OTHER DELAMINATION MODELS

Adhesion between solid bodies has been extensively investigated since the development of the successful Johnson-Kendall-Roberts (JKR) and Derjaguin-Muller-Toporov (DMT) models [14, 15]. However, these earlier models do not apply to thin films because the plate-bending and membrane-stretching deformation modes are vastly different from Hertz's contact problem, where stress at the contact interface is compressive, instead of tensile. In Wan's "punch" test, a circular membrane clamped at its perimeter is adhered to a rigid cylindrical punch [16-18] (Figure 1.4). When the punch is pulled away by an external tensile load, the contact circle contracted and vanished at a critical load and punch displacement. A theoretical model is derived and verified experimentally for the interfacial delamination process with a film undergoing mixed bending and stretching deformation and zero residual stress. Wan and Kogut [19] further derived an elastic model for a flexible stretching membrane with zero flexural rigidity and, therefore, zero bending moment. A range of residual membrane stresses is considered.

Figure 1.4. Axisymmetric Film and Cylindrical Punch

1.4. MOTIVATION AND OBJECTIVE OF THIS RESEARCH

Film-substrate delamination for residual stress-free 1-D linear and 2-D axisymmetric models has been discussed with different assumptions in Wan's work [16, 17, 19-22]. In this chapter, the same 1-D and 2-D configurations are considered, and films in both models are treated as a stiff plate where bending deformation is the only dominant mode of deformation. The incremental membrane stress, or concomitant stress, induced by the deformed film profile is ignored here, but a constant tensile residual membrane stress is introduced. Effects of the coupled interfacial adhesion and residual stress are investigated. The models are relevant to a number of MEMS devices and cell membranes.

1.5. FRACTURE MECHANICS – ENERGY CONSIDERATION

To understand why a specific contact area withstanding an external load up to certain point before a delamination being triggered at the contact front, it is important to study the energy of the system. System energy in the forms of external loading exists as potential energy, deformation of the film as elastic energy, and surface energy when new surface is created due to delamination. This concept is useful in understanding both experimental and theoretical model. When an external force is applied to the work piece, a displacement is produced and work is done, U_P, on the work piece. Under a fixed load condition, the energy of the system is given by [23]

$$-\text{ work done by the external force} + \text{increase in strain energy of the body} \tag{1.1}$$

$$-F\,\delta w_0 + \tfrac{1}{2}F\,\delta w_0 \tag{1.2}$$

In this thesis, stain energy of the body is represented as U_E. If there is a crack extension or delamination between layers within the work piece, energy is released as a result of the relaxation process, energy, *Us*, is required to produce the crack growth at each tip. U_S is considered as a constant for each increment of the crack or delamination length. *Us* takes a opposite sign than U_P because U_S is a result of U_P. By summing all the separate energies, the curve representing the total energy of the system is obtained as illustrated in Figure 3.2. There is evident that decrease in contact area in the region $0 \leq c$

$\leq c_{equalibrium}$ requires an energy input to the system. However, for c > $c_{equalibrium}$ energy is released as a result of decrease in contact area.

1.6. PLATE AND SHELL BENDING THEORY [24]

1.6.1. Cylindrical Bending of Uniformly Loaded Rectangular Plate with Clamped Edges. The author's 1-D adhesion-delamination model was derived based on the Timoshenko's "Cylindrical Bending of Uniformly Loaded Rectangular Plate with Clamped Edges" model (see Figure 1.5), with different boundaries conditions. The governing equation of this model is given

$$M = \frac{ql}{2}x - \frac{qx^2}{2} - \sigma h\ w + M_0 \tag{1.3}$$

where M is bending moment at any cross section of the film; q is the uniform pressure loading over the surface of the film, and $\sigma\ h$ is the tensile force. Substitute

$$\kappa\ \frac{d^2w}{dx^2} = -M \tag{1.4}$$

into Equation (1.3) and

$$\kappa\frac{d^2w}{dx^2} - \sigma h\ w = -\frac{qlx}{2} + \frac{qx^2}{2} - M_0 \tag{1.5}$$

would be obtained. Differentiate Equation (1.5) in term of x twice and the governing equation

$$\kappa\frac{d^4w}{dx^4} - \sigma h\frac{d^2w}{dx^2} = q \tag{1.6}$$

is derived and used as the governing equation as (2.1). In the author's model, external load is not applied as a uniform pressure. Instead, it is a shear force at the film/punch contact edge. Therefore, q in Equation (1.6) is replaced by $F\delta(x)$ and result in the governing equation given in (2.1).

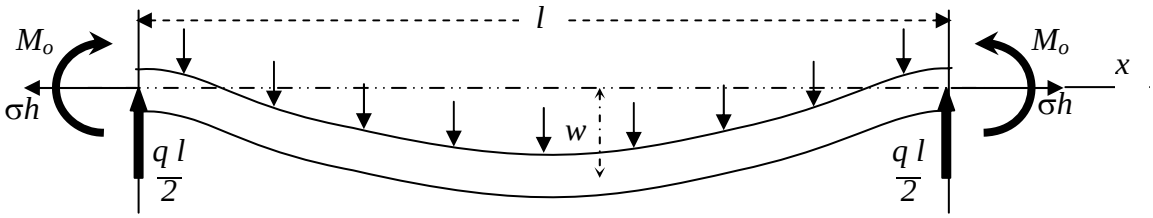

Figure 1.5. Cylindrical Bending of Rectangular Plate with Fixed Ends

1.6.2. Symmetrical Bending of the Circular Plate. Timoshenko's symmetrical bending model (Figure 1.6) of the circular plate considered both tangential and radial bending moment, M_t and M_r, respectively. The relation of tangential and radial bending moment per unit length to the plate profile at any point of the plate is given as

$$M_r = -\kappa\left(\frac{d^2w}{dr^2} + \frac{v}{r}\frac{dw}{dr}\right) \tag{1.7}$$

$$M_t = -\kappa\left(\frac{1}{r}\frac{d^2w}{dr^2} + v\frac{dw}{dr}\right) \tag{1.8}$$

Q is a shear force per unit length at the cylindrical section of radius r, which is replaced by $F/2\pi r$ in author's model, as the shear force is concentrated at the contact edge ($r=c$). The sum of all moments and shear force for an element in the circular plate "abcd," as in Figure (1.6) with proper signs is given to be

$$\underbrace{\left(M_r + \frac{dM_r}{dr}dr\right)(r+dr)d\theta}_{\text{Radial Bending at 'a b'}} - \underbrace{M_r r\, d\theta}_{\substack{\text{Radial Bending}\\ \text{at 'c d'}}} - \underbrace{M_t\, dr\, d\theta}_{\substack{\text{Tangential Bending}\\ \text{at 'a d' and 'b c'}}}$$

$$- \underbrace{\sigma h\, r\, d\theta\, dr\frac{dw}{dr}}_{\substack{\text{Tensile}\\ \text{Stress}}} + \underbrace{Qr\, d\theta\, dr}_{\substack{\text{Shear force}\\ \text{at the element}}} = 0 \tag{1.9}$$

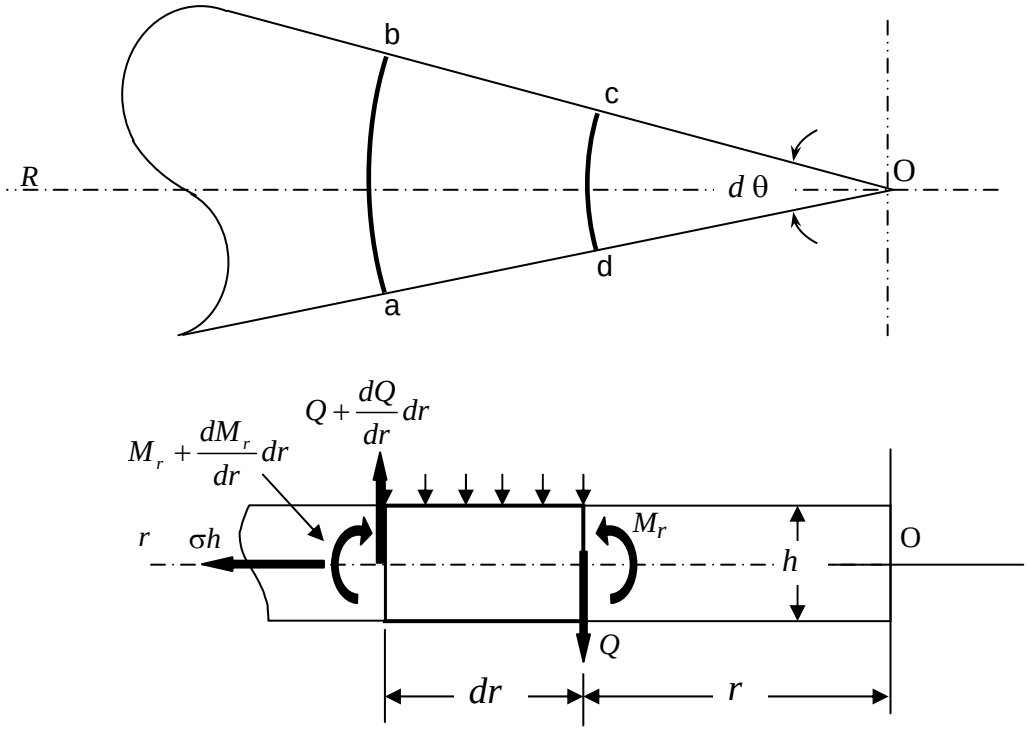

Figure 1.6. Timoshenko's Symmetrical Bending Model. (Above) An Element of Symmetrical Bending of the Circular Plate, 'abcd.' (Below) Cross-Section of the Element

By neglecting the small quantity of higher order and substituting the expression from , (1.7) and (1.8), (1.9) becomes (1.10)

$$\kappa\left(\frac{d^3w}{dr^3}+\frac{1}{r}\frac{d^2w}{dr^2}-\frac{1}{r^2}\frac{dw}{dr}\right) - \sigma h\left(\frac{dw}{dr}\right) = Q \tag{1.10}$$

where Q is the share force at the contact edge and can be expressed as $F/ 2\pi r$.

2. FILM-SUBSTRATE DELAMINATION OF 1-D RECTANGULAR PLATE

2.1. MODEL AND ASSUMPTIONS

Film-substrate delamination is a delamination process of a film from a punch substrate. The 1-D model, as illustrated in Figure 2.1, is a rectangular model such that the coordinate of the system can be considered to be a straight line in one direction x. The rectangular film with thickness h, elastic modulus E, Poisson's ratio ν, bending rigidity $\kappa = Eh^3 / 12(1-\nu^2)$, and tensile residual stress σ_0, is clamped at both ends and in contact with a punch substrate where the contact surface energy is Γ. Under this situation, the clamped section of the film is assumed to be fixed and no side sliding will occur at any time.

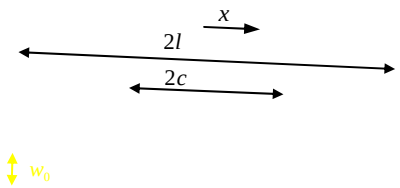

F

Figure 2.1. 1-D Rectangular Film/Substrate Delamination Model

When an external force is applied to the punch substrate to the film surface in the normal direction, the punch will move away from the film and will cause the film-punch delamination and deformation of the film at the over-hanging section. Assuming the film is a stiff plate (large E) such that the film is undergoing bending deformation, tensile

stress of the film will be dominated by residual stress, so that $\sigma \approx \sigma_0$ with film profile, $w(x)$. Once F reaches a critical load, a delamination is driven into the film-substrate interface with an adhesion energy, γ, and the contact length shrinks to c ($< l$). Without delamination (constant c), the film deformation is governed as shown in (2.1)

$$\underbrace{\kappa \nabla^4 w}_{\text{Plate-bending}} - \underbrace{\sigma_0 h \nabla^2 w}_{\substack{\text{Membrane-stretching} \\ \text{due to residual stress}}} = \underbrace{F \delta(x)}_{\text{Central external load}} \tag{2.1}$$

where $\nabla^2 \equiv \partial^2 / \partial x^2$ is the Laplacian operator in the 1-D Cartesian coordinate system, and $\delta(x)$ is the Dirac delta function denoting the applied force loading acting at the contact edge. In fact, the actual mechanical force on the membrane is concentrated at the contact edge or $F\,\delta(c)$, but it is mathematically equivalent to write $F\,\delta(x)$.

2.2. SOLVING GOVERNING EQUATION

Because the 1-D linear model is symmetric about the center of the film where the origin of the coordinate system lies, only one side of the model is considered for calculation. Within the contact ($x < c$), the film is planar, which implies $w = w_0$ and $dw/dx = 0$. The integration of Equation (2.1) is

$$\kappa \frac{\partial^3 w}{\partial x^3} - \sigma_0 h \frac{\partial w}{\partial x} = \frac{F}{2} \tag{2.2}$$

where F is the force applied to the punch per unit width. The first term corresponds to the bending deformation of the overhanging film, where $c < x < l$, and the second term corresponds to the stretching deformation at the same region due to residual stress. A set of normalized variables, $\omega = w/h$, $\xi = x/l$, $\beta = (l^2 h / \kappa)^{1/2} \sigma_0^{1/2}$, and $\varphi = (l^3 / 2\kappa h) F$, will be adopted for simplicity. The equation is then

$$\frac{\partial^3 \omega}{\partial \xi^3} - \beta^2 \frac{\partial \omega}{\partial \xi} = \varphi \tag{2.3}$$

The boundary conditions are given by $(\partial\omega/\partial\xi) = 0$ at the contact edge ($\xi = \lambda$) and at the clamps ($\xi = 1$), and $\omega = 0$ at $\xi = 1$. The solution of (2.3) is

$$\omega = \frac{\varphi}{\beta^3}\left\{\left(\frac{1}{e^{\beta\lambda}+e^{\beta}}\right)e^{\beta\xi} - \left(\frac{e^{\beta(\lambda+1)}}{e^{\beta\lambda}+e^{\beta}}\right)e^{-\beta\xi} + \beta\,(1-\xi) + \frac{e^{\beta\lambda}-e^{\beta}}{e^{\beta\lambda}+e^{\beta}}\right\} \tag{2.4}$$

with vertical displacement at $\xi = \lambda$,

$$\omega_0 = \omega\,|_{\xi=\lambda} = \varphi\left\{-\frac{2}{\beta^3}\tanh\left[\frac{\beta}{2}(1-\lambda)\right] + \frac{1}{\beta^2}(1-\lambda)\right\} \tag{2.5}$$

The first two exponential terms in Equation (2.4), $e^{\beta\xi}$ and $e^{-\beta\xi}$, and the hyperbolic tangent term in (2.5) are the result of the bending moments at the clamps and the contact edges (c.f. first term in (2.2) and (2.3)). For a fixed contact area (λ = constant), the constitutive relation in Equation (2.5) is linear with $\varphi \propto \omega_0$, and the proportionality constant (the curly bracket in (2.5)) depends on β and λ only.

2.3. ENERGY BALANCE OF THE DELAMINATION SYSTEM

2.3.1. Delamination Event and Energy Balance. The delamination process is investigated by an energy balance. Once the external force loading reaches a certain threshold, delamination is driven into the contact surface from both ends of the film toward the center. The total energy, U_T, of the film-punch system consists of three elements

$$U_T = U_P + U_E + U_S \tag{2.6a}$$

where potential energy, U_P, elastic energy, U_E, and surface energy, U_S are

$$U_P = F\ w_0$$

$$U_E = -\int_0^{w_0} F\ dw_0 = -\tfrac{1}{2}\ F\ w_0$$

$$U_S = 2\ \gamma\ c \qquad (2.6b)$$

Due to the linear relation of $\varphi \propto \omega_0$, the integration of U_E can be reduced to $-\frac{1}{2}\ F\ w_o$. (2.6a) and (2.6b) can be normalized using the relationship $\Sigma_T = (l^2/2\kappa h^2)\ U_T$. Thus, the total energy of the system and its elements would be,

$$\Sigma_T = \Sigma_P + \Sigma_E + \Sigma_S \qquad (2.7a)$$

$$\Sigma_P = \varphi\ \omega_0$$

$$\Sigma_E = -\int_0^{w_0} \varphi\ d\omega_0 = -\tfrac{1}{2}\ \varphi\ \omega_0$$

$$\Sigma_S = \Gamma\ \lambda \qquad (2.7b)$$

2.3.2. Delamination Trajectory in Terms of Energy. Delamination occurs when $\partial U_T / \partial c \geq 0$. At equilibrium, when the equals sign holds,

$$\gamma = -\frac{\partial}{\partial c}\left(\frac{1}{2}\ F\ w_0\right)_{F=\text{constant}} \qquad (2.8)$$

In order to normalize the variables for simplicity, $\omega = w/h$ and $\varphi = (l^3/2\kappa h)\ F$ to Equation (2.8), so that $\Gamma = (l^4/kh^2)$ and

$$\Gamma = -\frac{\partial}{\partial\lambda}\left(\frac{1}{2}\ \varphi\ \omega_0\right)_{\varphi=\text{constant}} = -\frac{\varphi}{2}\left(\frac{\partial\omega_0}{\partial\lambda}\right)$$

$$= \frac{\varphi^2}{2\ \beta^3}\ \frac{\partial}{\partial\lambda}\left\{\ 2\ \tanh\left[\frac{\beta}{2}(1-\lambda)\right]\ -\ \beta\ (1-\lambda)\ \right\}$$

$$= \left\{\frac{1}{2\beta^2}\tanh^2\left[\frac{\beta(1-\lambda)}{2}\right]\right\}\ \varphi^2 \qquad (2.9)$$

As delamination proceeds, the contact area shrinks from both ends toward centers of the punch until condition in the (2.9) is satisfied. In summary, Table 2.1 lists the conversions between all the variables and their corresponding normalized variable.

Table 2.1. Normalized Variables used in the 1-D Film-Substrate Delamination Model

	Physical Parameters	**Normalized Parameters**
Geometrical Parameters	w = deformation profile h = film thickness l = film length c = length of contact area	$\omega = w/h$ $\xi = x/l$ $\lambda = c/l$
Material Parameters	E = elastic modulus ν = Poisson's ratio κ = flexural rigidity = $E\,h^3 / 12\,(1-\nu^2)$ γ = interfacial adhesion energy ($J.m^{-2}$) σ_0 = tensile residual stress ($N.m^{-2}$)	$\Gamma = \left(\frac{l^4}{\kappa h^2}\right)\gamma$ $\beta = \left(\frac{l^2 h}{\kappa}\right)^{1/2}\sigma_0^{1/2}$
Mechanical Loading	F = applied external force w_0 = vertical displacement of punch U_T = total energy of film-punch system	$\varphi = \frac{l^3}{2\kappa h}F$ $\omega_0 = \frac{w_0}{h}$ $\Sigma_T = \frac{l^3}{2\kappa h^2}U_T$

Rewriting (2.9) as $\varphi(\lambda)$

$$\varphi = \sqrt{2\,\beta^2\,\Gamma}\,\coth\left[\frac{\beta(1-\lambda)}{2}\right] \tag{2.10}$$

It is logical to consider φ as a function of λ because the external force will never be a factor of the size of the contact area, but the size of the contact area affects the equilibrium external force.

2.4. CONSTITUTIVE RELATION

At every equilibrium stage of delamination, the punch displacement is related to the contact length by eliminating φ from Equation (2.5) and (2.10)

$$\omega_0 = \sqrt{2\,\beta^2\,\Gamma}\left\{\frac{1-\lambda}{\beta^2}\coth\left[\frac{\beta}{2}(1-\lambda)\right]-\frac{2}{\beta^3}\right\} \tag{2.11}$$

The general delamination trajectory for any Γ and β can be found by eliminating λ from Equation (2.5) and (2.10) and becomes

$$\varphi = \sqrt{2\,\beta^2\,\Gamma}\,\coth\left[\frac{1}{\varphi}\left(\frac{\beta^3\omega_0}{2}+\sqrt{2\,\beta^2\,\Gamma}\right)\right] \tag{2.12}$$

which is a transcendental function involving φ on both sides of the equation. The asymptotic behavior will be discussed later. As for now, to circumvent the mathematically formidable task, $\varphi(\omega_0)$ can be found as a log-log parametric plot with a fixed Γ and β and a varying λ. If the constitutive relation is cast in the form of $\varphi \propto (\omega_0)^n$ as in Wan's earlier work [16, 21],then the gradient of $\varphi(\omega_0)$ in a log-log graph is given by

$$n = \frac{\partial(\log\varphi)}{\partial(\log\omega_0)} = \frac{\omega_0}{\varphi}\left(\frac{\partial\varphi/\partial\lambda}{\partial\omega_0/\partial\lambda}\right) = \frac{2\tanh\left[\beta(1-\lambda)/2\right]-\beta(1-\lambda)}{\sinh\left[\beta(1-\lambda)\right]-\beta(1-\lambda)} \tag{2.13}$$

Here $n(\beta,\lambda)$ is independent of Γ and is confined by $-½ \le n \le 0$. The independence of Γ is because Γ is a coefficient of $\varphi(\beta, \lambda)$ and $\omega_0(\beta, \lambda)$ (see Equations (2.10) and (2.11)) and is canceled out in Equation (2.13). Thus, delamination behavior will not be affected by residual stress. The lower limit corresponds to the dominant bending moments ($\beta \to 0$

and $\varphi \propto \omega_0^{-1/2}$), while the upper limit denotes the dominant residual stress ($\beta \to \infty$ and φ = constant).

Two limiting cases for $\beta = 0$ and $\beta \to \infty$ are derived. For a film free of residual stress ($\beta = 0$), (2.10) and (2.11) reduce to

$$\varphi\big|_{\beta=0} = \frac{\sqrt{8}}{1-\lambda}\,\Gamma^{1/2} \tag{2.14}$$

$$\omega_0\Big|_{\beta=0} = \frac{(1-\lambda)^2}{\sqrt{18}}\,\Gamma^{1/2}, \tag{2.15}$$

respectively. The external load diminishes with the contact area (i.e., decreasing λ) and reaches its minimum at $(8\,\Gamma)^{1/2}$ when $\lambda = 0$. However, one ambiguity exists with Equation (2.14). If the punch substrate has the same length as the film, then the applied load at the delamination initiation stage ($\lambda \to 1$), $\varphi|_{\beta=0}$ approaches infinity, which is non-physical. For the same situation in real life, the film is under pure shear loading at the contact edge, which is not considered in the model. The discrepancy is the result of the assumption that the film has a uniform bending moment along its thickness. For a very short delamination length compared with the film thickness, $(l - c) >> h$, the stress field is confined to the vicinity of the delamination front, reminiscent of a small crack in a continuum solid. Equation 2.1, therefore, breaks down, and the subsequent calculation becomes invalid. Because a practical punch in an experiment must be shorter than the film span, the mathematical singularity is ignored in the following discussion. Eliminating λ from (2.14) and (2.15), the mechanical response reduces to

$$\varphi\big|_{\beta=0} = \left[\left(\frac{32}{9}\right)^{1/4}\Gamma^{3/4}\right]\frac{1}{\omega_0^{1/2}} \tag{2.16}$$

which is consistent with (2.13) and implies $\varphi \propto \omega_0^{-1/2}$. Experiments can only be conducted in the fixed-grips (i.e., displacement-controlled) configuration to maintain

stable equilibrium at all λ. It can easily be shown that $\partial^2\Sigma_T/\partial\lambda^2 < 0$ using 2.10, which warrants stability for fixed ω_0. In the limit of $\beta \to \infty$, Equations 2.10 and 2.11 reduce to

$$\varphi\,|_{\beta\to\infty} = \sqrt{2\,\beta^2\,\Gamma} \tag{2.17}$$

$$\omega_0\big|_{\beta\to\infty} = \frac{\sqrt{2\,\Gamma}}{\beta}(1-\lambda)\,, \tag{2.18}$$

respectively. Equation (2.15) requires the delamination load to be constant and independent of the simultaneous contact length as long as Γ and β are fixed. Practically, when the punch is pulled from the film in a fixed-grip configuration, the applied load stays constant until the contact area gradually and stability shrinks and ultimately reduces to a line ($\lambda = 0$). Then the film separates completely from the punch. The delamination process is technically a neutral equilibrium [25], i.e., $\partial^2\Sigma_T/\partial\lambda^2 = 0$. If a fixed-load is chosen, then once the load reaches the critical threshold, delamination will initiate and continue spontaneously until the entire contact area vanishes.

Figure 2.2 shows the delamination trajectory ABCD for $\Gamma = 1$ and $\beta^2 = 100$. When the punch displacement is small along path AB, $\varphi(\omega_0)$ approximates Equations (2.12) and (1.13), and $n \approx -½$. Further movement of the punch leads to path CD with $\omega_0 > 0.01$ where the external load stays constant following (2.15) and $n \approx 0$. At D, the terminal point along the delamination curve, the contact reduces to a line with $\lambda^* = 0$, and the film pinches off the substrate at φ^* and $\omega_0{}^*$ with the asterisk denoting "pinch-off" hereafter. At D

$$\omega_0{}^* = \sqrt{2\,\beta^2\,\Gamma}\left[\,\frac{1}{\beta^2}\coth\!\left(\frac{\beta}{2}\right) - \frac{2}{\beta^3}\,\right] \tag{2.19}$$

by putting $\lambda = 0$ in (2.11). The bending-stretching transition occurs along path BC and can be approximated by the intersection of (2.16) and (2.17)

$$\omega_0{}^{\#} = \left(\frac{8}{9}\right)^{1/2}\frac{\Gamma^{1/2}}{\beta^2} \tag{2.20}$$

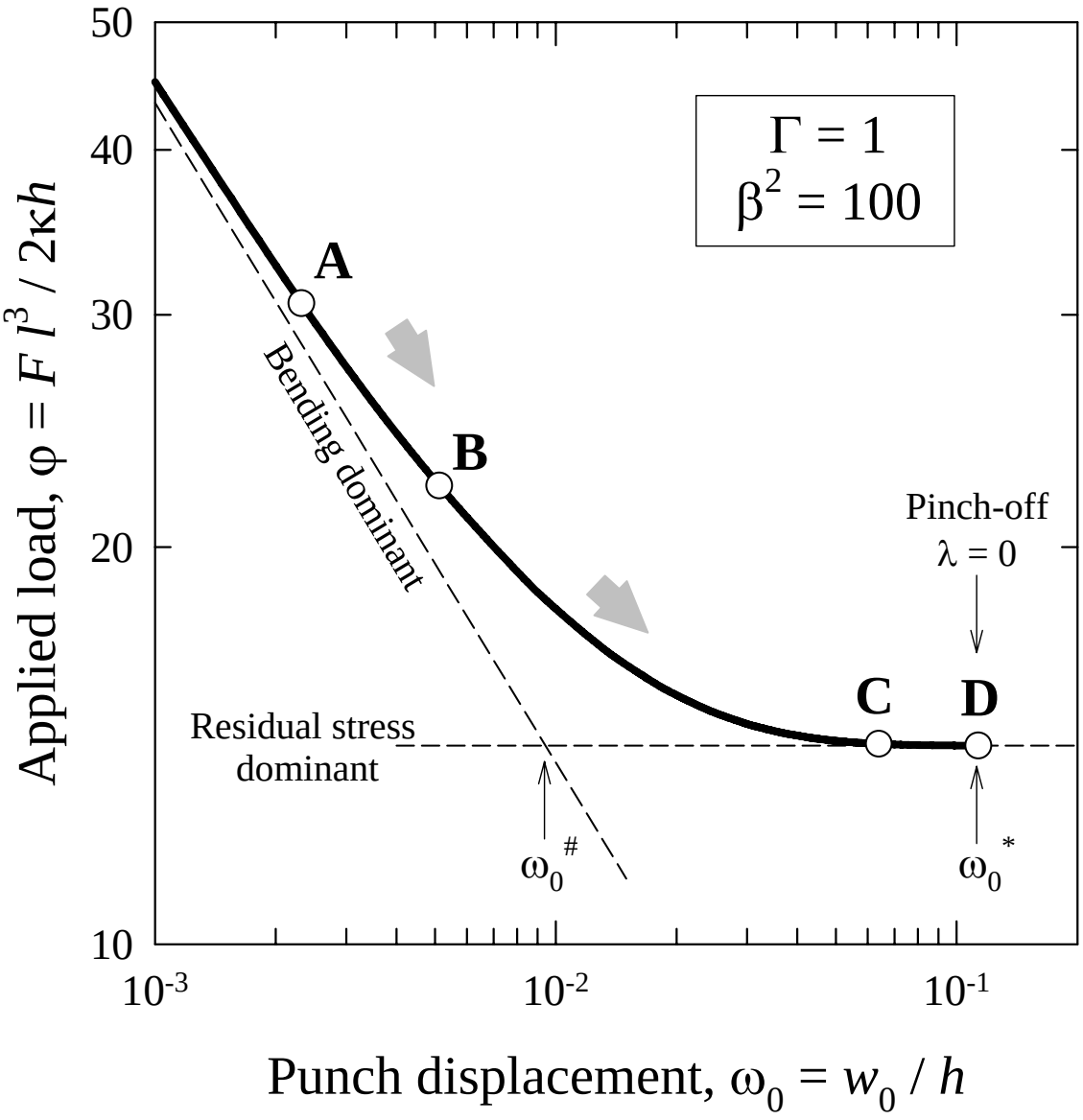

Figure 2.2. 1-D Constitutive Relation Delamination Trajectory

Film-punch substrate delamination depends on the amount of residual stress. Films with small residual stress possess large ω_0 ($>\omega_0^*$), and "pinch-off" takes place under bending deformation prior to any membrane stretching. Figure 2.3 shows $\varphi(\omega_0)$ for a fixed Γ and a range of β. All curves in Figure 2.3 terminate at "pinch-off" ($\omega_0 = \omega_0^*$ and $\lambda = 0$). For $\beta = 0$, $\varphi(\omega_0)$ strictly follows Equation (2.16) with $n = -½$. For a larger β and

$\omega_0 < \omega_0^*$, the deviation of $\varphi(\omega_0)$ from Equation (2.17) and (2.18) exacerbates and φ^* increases at a diminishing ω_0^* as shown by the dashed curves.

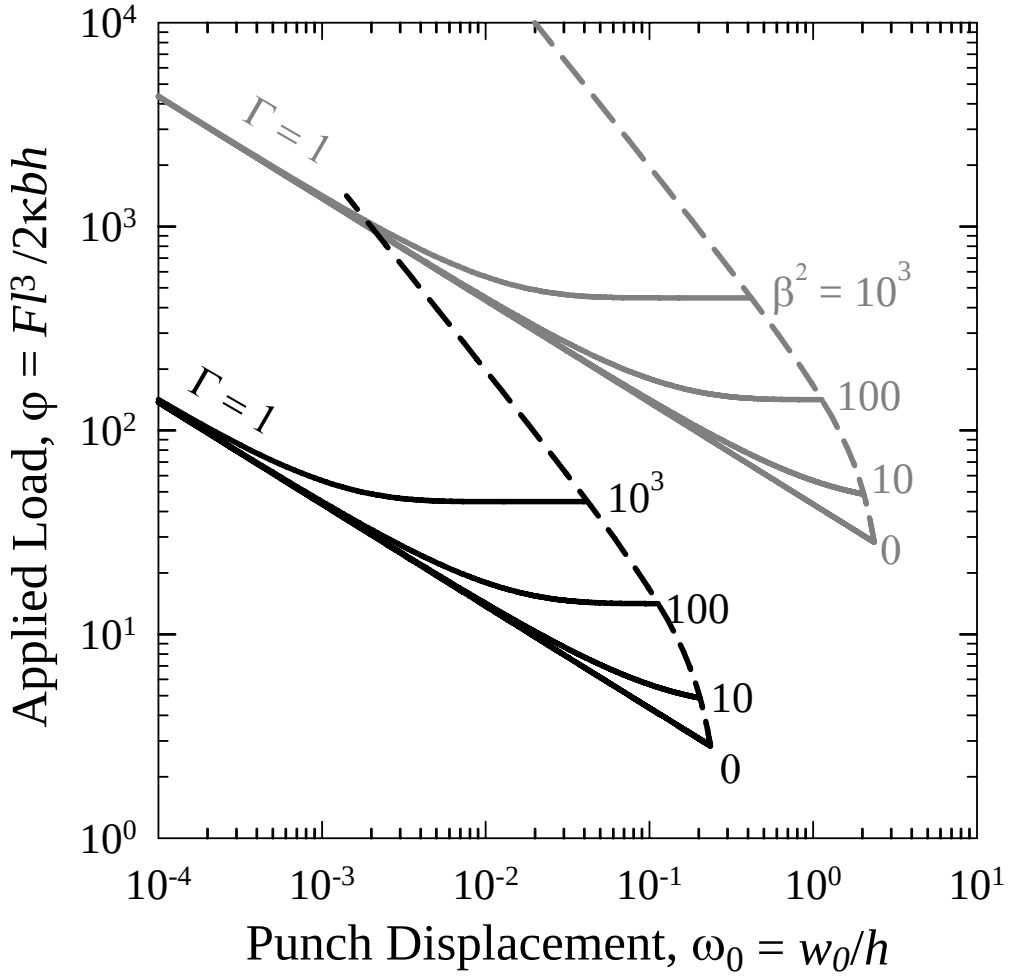

Figure 2.3. The 1-D Constitutive Relation Delamination Trajectories under Ranges of Residual Stress and Interfacial Adhesion Energy

In the limit of $\beta \rightarrow \infty$, $\varphi(\omega_0)$ approaches the asymptote in Equation(2.19). Increasing Γ translates the family of $\varphi(\omega_0,\beta)$ curves to higher values of φ and ω_0. Figure 2.4 shows the gradient *n* as a function of λ for a range of β and any value of Γ, with $-½ \leq$

$n \leq 0$. As discussed in the previous section, n is independent to Γ. Delamination proceeds from right to left with a decreasing λ and is indicated by the arrow. At the delamination initiation stage ($\lambda = 1$ and $\omega_0 = 0$), $n = -½$. At "pinch-off" ($\lambda = 0$ and $\omega_0 = \omega_0^*$), n varies between 0 (for $\omega_0 < \omega_0^{\#}$) and $-½$ (for $\omega_0 > \omega_0^{\#}$) depending on the value of β. The trajectory ABCD corresponds to ABCD in Figure 2.2.

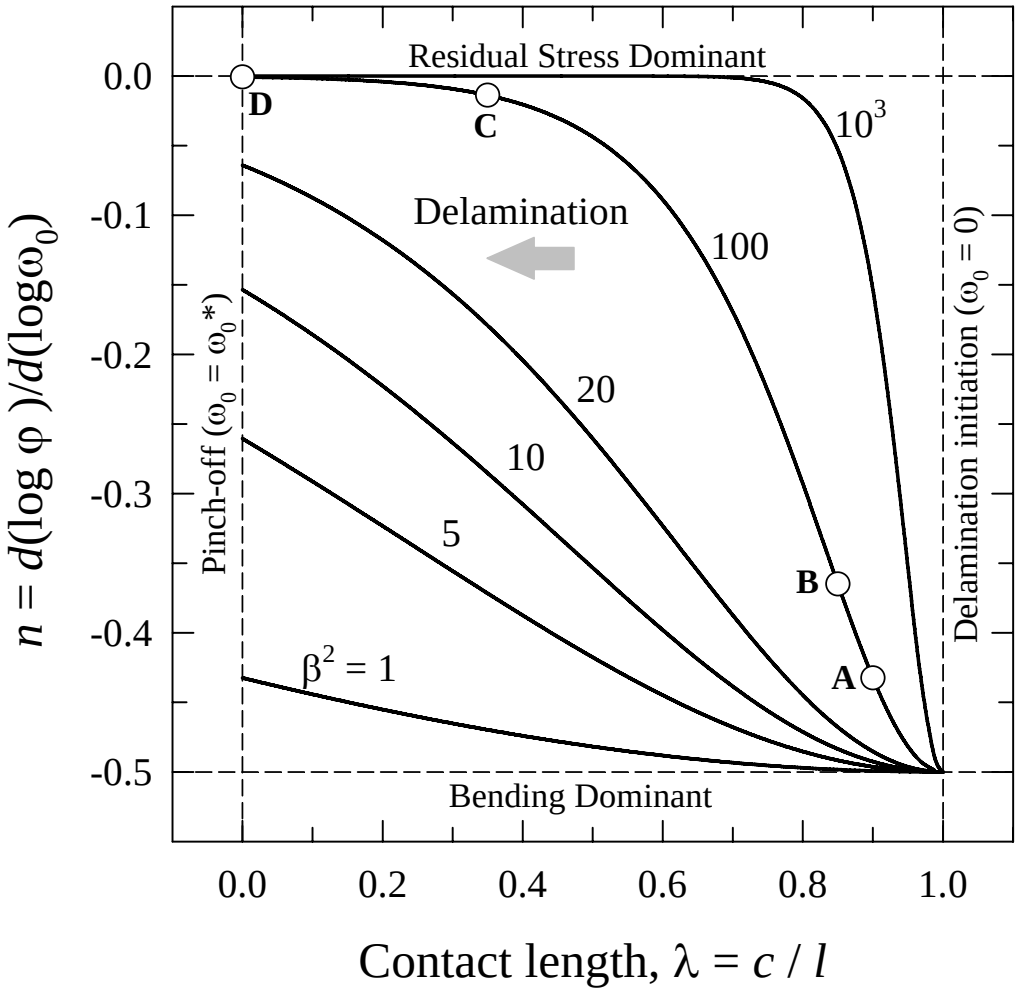

Figure 2.4. Gradient of Delamination Trajectory n versus Contact Length c with a Range of Residual Stress β^2

3. FILM-SUBSTRATE DELAMINATION OF 2-D AXISYMMETRIC PLATE

3.1. MODEL AND ASSUMPTION

In this section, the film of the axisymmetric model is assumed to be a stiff plate. Therefore, deformation of the film would be mostly bending, and concomitant stretching would be negligible. This assumption is the same as the rectangular model in Section 2. Figure 3.1 shows a circular film with a radius, a, thickness, h, elastic modulus, E, Poisson's ratio, ν, bending rigidity, $\kappa = Eh^3 / 12(1-\nu^2)$, and tensile residual stress, σ_0, clamped at the perimeter. The film is brought into adhesive contact with the planar surface of a rigid cylindrical punch with a radius slightly smaller than a. The film-punch interface has an adhesion energy, γ, and the initial contact radius is a. An external tensile force, F, is applied to the cylindrical punch substrate. The film profile, $w(r)$, is deformed by plate-bending (Figure 3.1).

Figure 3.1. Axisymmetric Model with Plate-Bending Deformation

At a critical load and punch displacement, delamination is driven into the film-substrate interface, and the contact radius contracts to c (< a). The force-displacement relation without delamination incorporates the delamination mechanics. The deformation profile of the freestanding annulus ($c \le r \le a$) around the contact circle, $w(r)$, is governed by von Karman's equation [16],

$$\underbrace{\kappa\,\nabla^4 w}_{\text{Plate-bending}} - \underbrace{\sigma\, h\,\nabla^2 w}_{\text{Membrane-stretching}} = \underbrace{F\,\delta(r)}_{\text{Central external load}} \tag{3.1}$$

with $\nabla^2 = \frac{1}{r}\frac{\partial}{\partial r}(r\frac{\partial}{\partial r})$, the Laplacian operator in cylindrical coordinates for axisymmetric configuration; $\delta(r)$, the Dirac delta function denoting the applied load acting at the contact edge, and σ, the total membrane stress on the film. Because the film is under plate-bending deformation, it is assumed the $\sigma \approx \sigma_0$ as the concomitant stress is essentially zero.

3.2. SOLVING VON KARMAN'S EQUATION

Within the contact ($r < c$), the film is planar, $w = w_0$ and therefore $dw/dr = 0$, implying zero mechanical force acting on the film. After integration, Equation (3.1) can be reduced to

$$\kappa\left(\frac{d^3w}{dr^3}+\frac{1}{r}\frac{d^2w}{dr^2}-\frac{1}{r^2}\frac{dw}{dr}\right) - \sigma h\left(\frac{dw}{dr}\right) = \frac{F}{2\pi\, r} \tag{3.2}$$

The right-hand side is the line force at the contact edge with a length of $2\pi r$. An alternative interpretation of (3.1) is that the central point load applied to the punch $F\,\delta(r)$ is distributed to a line load at the contact edge ($r = c$). A set of normalized variables including, $\omega = w/h$, $\xi = r/a$, and $\theta = (a/h)(dw/dr)$, is substituted into Equation (3.2). Thus,

$$\xi^2\frac{\partial^2\theta}{\partial\xi^2}+\xi\frac{\partial\theta}{\partial\xi}-(1+\beta^2\xi^2)\theta = \xi\varphi \tag{3.3}$$

is derived. Because of the bending deformation at the contact edge and clamped perimeter, the boundary conditions of (3.3) are $\theta(1) = \theta(\zeta) = 0$. Equation 3.3 is the modified Bessel equation [26], which gives

$$\theta = \varphi \left[C_1\, I_1(\beta\xi) + C_2\, K_1(\beta\xi) - \frac{1}{\beta^2 \xi} \right] \tag{3.4}$$

where I_n and K_n are the nth modified Bessel functions of the first and second kind, and C_1 and C_2 are constants to be fit to the boundary conditions:

$$C_1 = \frac{1}{\beta^2 \zeta} \left[\frac{K_1(\beta) - \zeta\, K_1(\beta\zeta)}{I_1(\beta)K_1(\beta\zeta) - I_1(\beta\zeta)K_1(\beta)} \right] \tag{3.5a}$$

$$C_2 = \frac{1}{\beta^2 \zeta} \left[\frac{I_1(\beta) - \zeta\, I_1(\beta\zeta)}{I_1(\beta)K_1(\beta\zeta) - I_1(\beta\zeta)K_1(\beta)} \right] \tag{3.5b}$$

The profile is found by integrating θ with respect to ξ to give

$$\omega = \frac{\varphi}{\beta} \left\{ C_1 \left[-1 + I_0(\beta\xi) \right] - C_2 K_0(\beta\xi) + C_3 - \frac{\log \xi}{\beta} \right\} \tag{3.6}$$

C_3 is a constant satisfying boundary condition at the perimeter, where $\omega(\xi) = 0$,

$$C_3 = \frac{1}{\beta^2 \zeta} \left[\frac{\left[I_0(\beta) - 1 \right] \left[K_1(\beta) - \zeta\, K_1(\beta\zeta) \right] + K_0(\beta)[I_1(\beta) - \zeta\, I_1(\beta\zeta)]}{I_1(\beta)K_1(\beta\zeta) - I_1(\beta\zeta)K_1(\beta)} \right] \tag{3.6b}$$

The vertical displacement of the punch, or in other words, the central displacement of the diaphragm, ω_0, is $\omega(\xi)$, and

$$\omega_0 \;=\; \omega\big|_{\xi=\zeta} \;= \frac{\varphi}{\beta} \left[C_1 \left[1 - I_0(\beta\zeta) \right] - C_2 K_0(\beta\zeta) + C_3 - \frac{\log \zeta}{\beta} \right] \tag{3.7}$$

Note that the relation, $F(w_0)$ or $\varphi(\omega_0)$, is *linear* (i.e., $\varphi \propto \omega_0$), because the square bracket in (3.7) is a constant depending only on the residual stress and the contact radius. This proportionality constant increases for a larger residual stress, leading to a stiffer film and a higher apparent elastic modulus. Similarly, a large punch gives rise to a narrower freestanding annulus and thus a less compliant system with a lower ω_0.

3.3. ENERGY BALANCE OF THE DELAMINATION SYSTEM

3.3.1. Delamination and Energy Balance. Once the applied tensile load exceeds a critical threshold, delamination drives into the film-substrate interface from the suspended annulus toward the center of the punch. The delamination mechanics are derived by a thermodynamic energy balance. The total energy of the punch-film system is given by

$$U_T = U_P + U_E + U_S \tag{3.8}$$

Similar to the 1-D model, the total energy of the film/punch system consists of three elements: potential energy, U_P, elastic energy, U_E, and surface energy, U_S:

$$\begin{aligned} U_P &= F\ w_0 \\ U_E &= -\int_0^{w_0} F\ dw_0 = -\tfrac{1}{2}\ F\ w_0 \\ U_S &= -2\pi\ c\ \gamma \end{aligned} \tag{3.9}$$

Due to the linear relation of $\varphi \propto \omega_0$, the integration of U_E can be reduced to $-\frac{1}{2}\ F\ w_o$. Equation (3.8) can be normalized using the relationship $\Sigma_T = (a^2/2\pi\kappa h^2)\ U_T$. Then, total energy of the system and its elements would be

$$\Sigma_T = \Sigma_P + \Sigma_E + \Sigma_S \tag{3.10a}$$

$$\Sigma_P = \varphi\ \omega_0$$

$$\Sigma_E = -\int_0^{w_0} \varphi\ d\omega_0 = -\tfrac{1}{2}\ \varphi\ \omega_0$$

$$\Sigma_S = -\Gamma\ \lambda \qquad (3.10b)$$

Substituting (3.10a) into (3.10b),

$$\Sigma_T = \tfrac{1}{2}\ \varphi\ \omega_0 - \zeta^2\ \Gamma \qquad (3.11)$$

Coupling of interfacial adhesion and residual stress is obvious when substituting (3.7) into (3.11).

3.3.2. Delamination Trajectory in Terms of Energy. As mentioned in Section 3.3.1, delamination occurs when an external load exceeds certain threshold. To demonstrate how (3.11) accounts for the thin film delamination, and the parameters are set to be $\Gamma = 1.00$ and $\beta = 1.00$. Figure 3.2 shows a family of $\Sigma_T(\zeta)$ for a range of ω_0. Assume the diameter of the punch is 0.5702 time of the film's, the punch can be raised from $\omega_0 = 0$ to 0.05, where a stable equilibrium at without delamination. Further increase occurs in the punch displacement to B', and the contact radius remain unchanged. The total energy of the system is at an unstable point and there is a tendency to push the system energy toward point B where contact radius ζ_B decrease from 0.5702 to 0.4464 as shown in Figure 3.2.

From a mathematical standpoint, delamination occurs when $(\partial\Sigma_T / \partial\zeta) \geq 0$. Figure 3.2, B' is at a point where $(\partial\Sigma_T / \partial\zeta) \geq 0$ and B is at a point where $(\partial\Sigma_T / \partial\zeta) = 0$. To derive the delamination trajectory, which is a series of equilibrium points, derive $(\partial\Sigma_T / \partial\zeta) = 0$ from (3.11) and get,

$$\Gamma = \frac{\varphi}{2}\left[\frac{d\omega_0}{d(\zeta^2)}\right]_{\varphi=\text{constant}} \qquad (3.12)$$

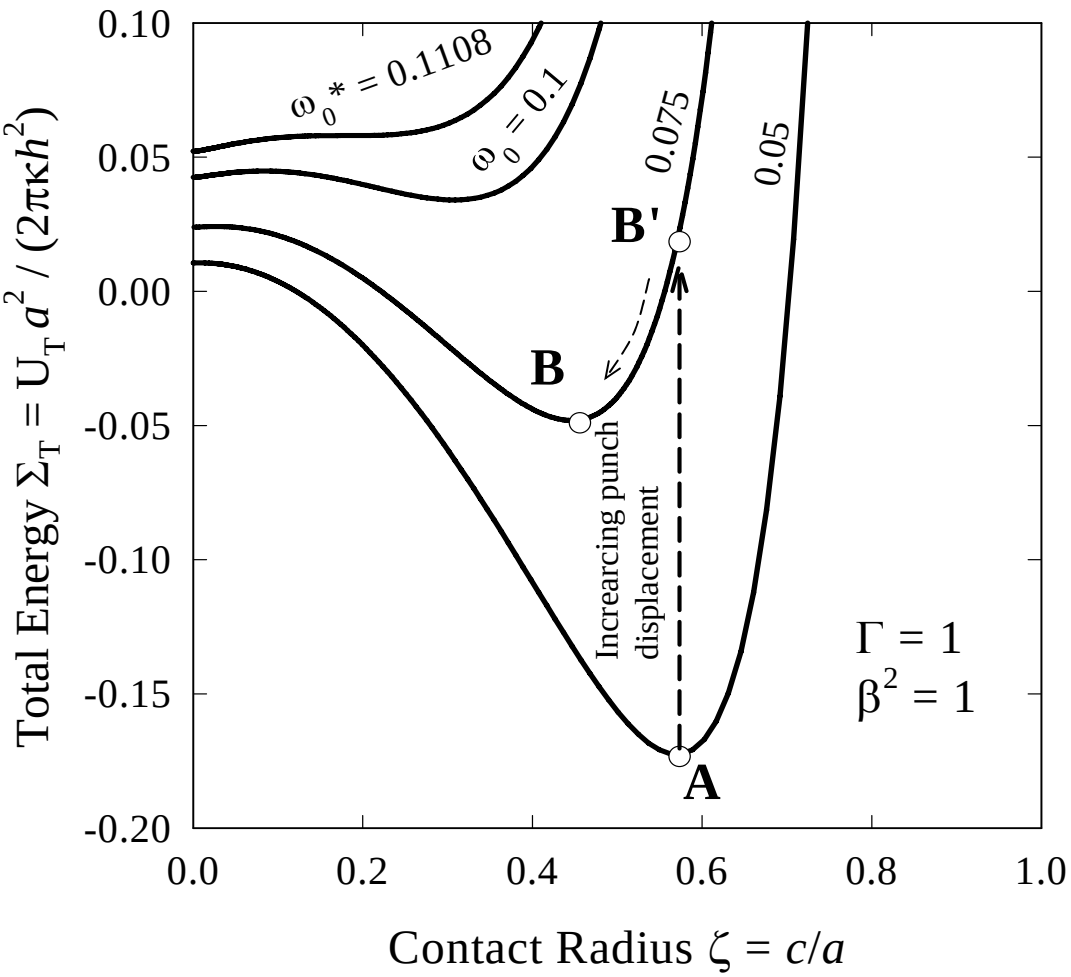

Figure 3.2. System Energy Tends to Settle at a Stable Equilibrium Point.

Figure 3.3 is the same plot as Figure 3.2 with a grey delamination trajectory. The grey trajectory connects all the minima (A-B-C) at different punch displacement levels and denotes the stable delamination trajectory. Ultimately when ω_0 reaches 0.1108, the two extrema merge to an inflexion at C with $(d^2\Sigma_T/d\zeta^2) = 0$, $\omega_0^* = 0.1108$, $\zeta^* = 0.1796$, and $\varphi^* = 1.6286$, resulting in a neutral equilibrium. An incremental increase from ω_0^* leads to a spontaneous "pull-off," the contact radius drops to zero ($\zeta = 0$), and the film snaps from the substrate. The dashed curve OC joining the maxima of $\Sigma_T(\zeta)$ is physically inaccessible and will be ignored.

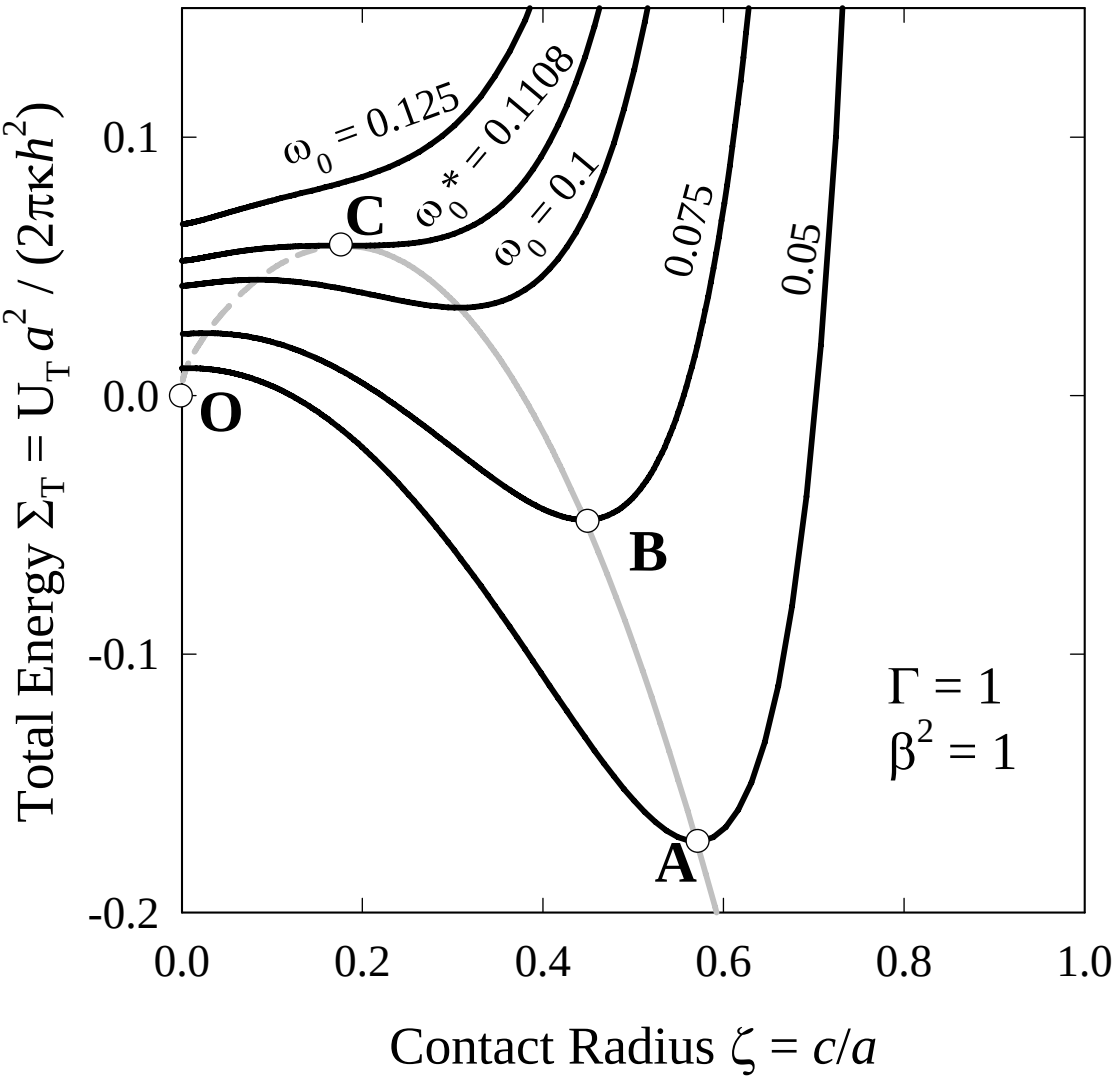

Figure 3.3. Delamination Trajectory of the System Energy (Grey Line)

Substituting (3.7) into (3.12),

$$\varphi = \left[2\beta\zeta \, \frac{I_1(\beta)K_1(\beta\zeta) - I_1(\beta\zeta)K_1(\beta)}{I_1(\beta)K_0(\beta\zeta) + I_0(\beta\zeta)K_1(\beta) - 1/\beta} \right] \Gamma^{1/2} \tag{3.13}$$

Equation (3.13) requires both φ and ω_0 to be proportional to $\Gamma^{1/2}$ (because $\varphi \propto \omega_0$ in (3.7)), and Γ can be factored out from the right hand side of (3.11). Because “pull-off”

requires $(\partial\Sigma_T/\partial\zeta) = 0$, once β is fixed, ζ^* is automatically determined and is therefore independent of Γ. When $(\partial\Sigma_T / \partial\zeta) < 0$, however, the film will not be adhered back onto the punch surface as the mathematical prediction. It is because the film would tend to release elastic stretching from the already deformed overhanging section rather than restoring surface energy by creating new adhered surface. At this point, all the normalized variables for the 2-D axisymmetric model have been introduced, and are summarized in Table 3.1.

Table 3.1. Normalized Variables Used in the 2-D Film-Substrate Delamination Model

	Actual Parameters	**Normalized Parameters**
Geometrical	$w(r)$ = deformation profile h = film thickness a = film radius c = radius of the film-substrate contact area	$\omega = \frac{w}{h}$, $\xi = \frac{r}{a}$, $\zeta = \frac{c}{a}$, $\theta = \frac{\partial\omega}{\partial\xi} = \frac{a}{h}\frac{\partial w}{\partial r}$
Material	E = elastic modulus ν = Poisson's ratio κ = flexural rigidity $= E\,h^3 / 12\,(1-\nu^2)$ γ = interfacial adhesion energy ($J.m^{-2}$) σ_0 = tensile residual stress ($N.m^{-2}$)	Adhesion Energy, $\Gamma = \left(\frac{a^4}{2\kappa h^2}\right)\gamma$, Residual Stress, $\beta = \left(\frac{a^2 h}{\kappa}\right)^{1/2}\sigma_0^{1/2}$
Mechanical Loading	F = applied external force w_0 = vertical displacement of the punch U_T = total energy of film-punch system	$\varphi = \frac{Fa^2}{2\pi\kappa h}$, $\omega_0 = \frac{w_0}{h}$, $\Sigma_T = \frac{a^2}{2\pi\kappa h^2}U_T$

3.3.3. Coupling Effect of Adhesion Energy and Residual Stress. The situation with a constant β with a varying Γ will be considered, followed by a constant Γ with a varying β. Figure 3.4 shows the stable trajectory of $\Sigma_T(\zeta)$ for β = 1 and a range of Γ. Each curve exercises a maximum corresponding to "pull-off" at $\zeta^* = 0.1796$ and the branch with $\zeta < \zeta^*$ (the area on the left-side of Figure 3.4) is physically inaccessible. The Γ-independency of ζ^* will be mathematically verified in the next section.

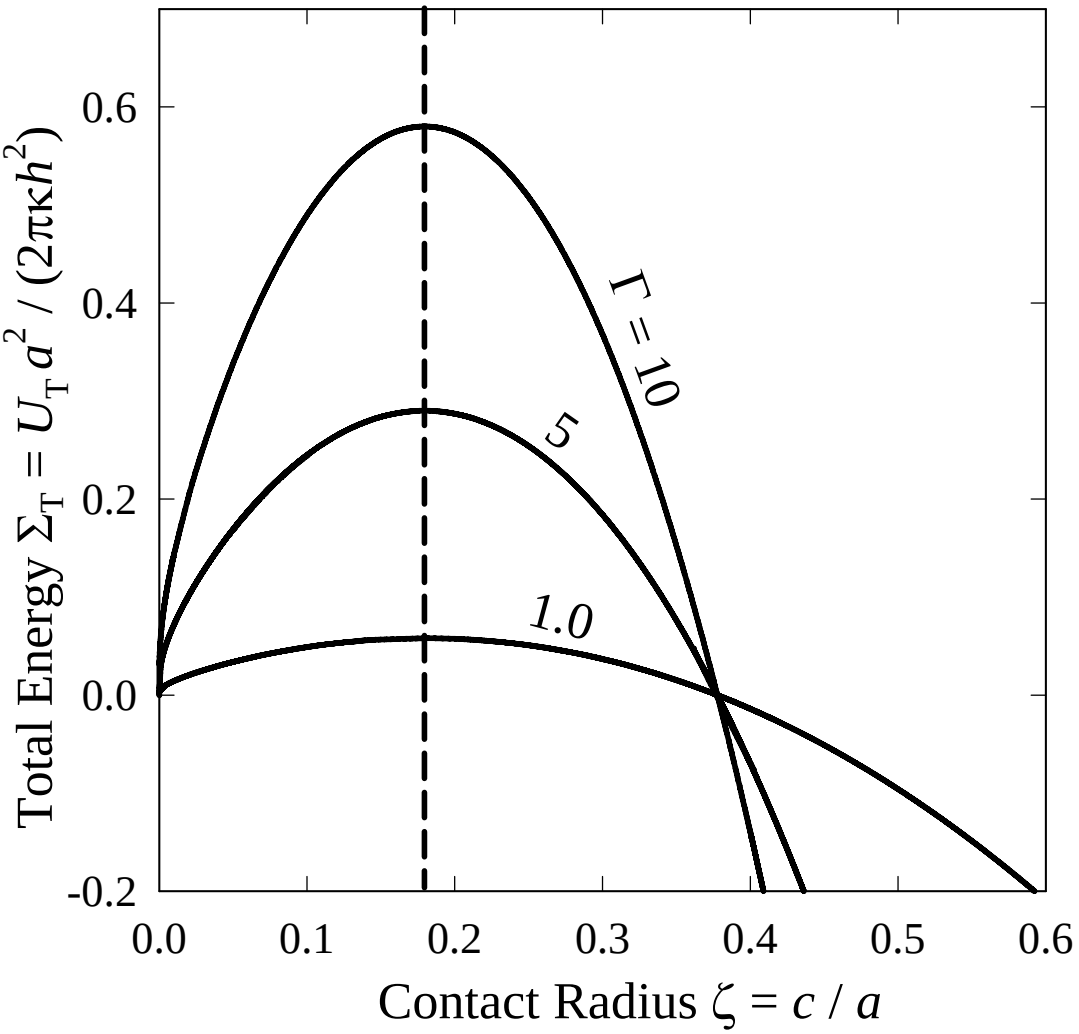

Figure 3.4. System Energy at a Range of Adhesion Energy

Next, assume Γ = 1 with a varying β, Figure 3.5 shows the stable delamination paths and "pull-off" at the maxima. As the residual stress increases, membrane stretching dominates and bending becomes negligible.

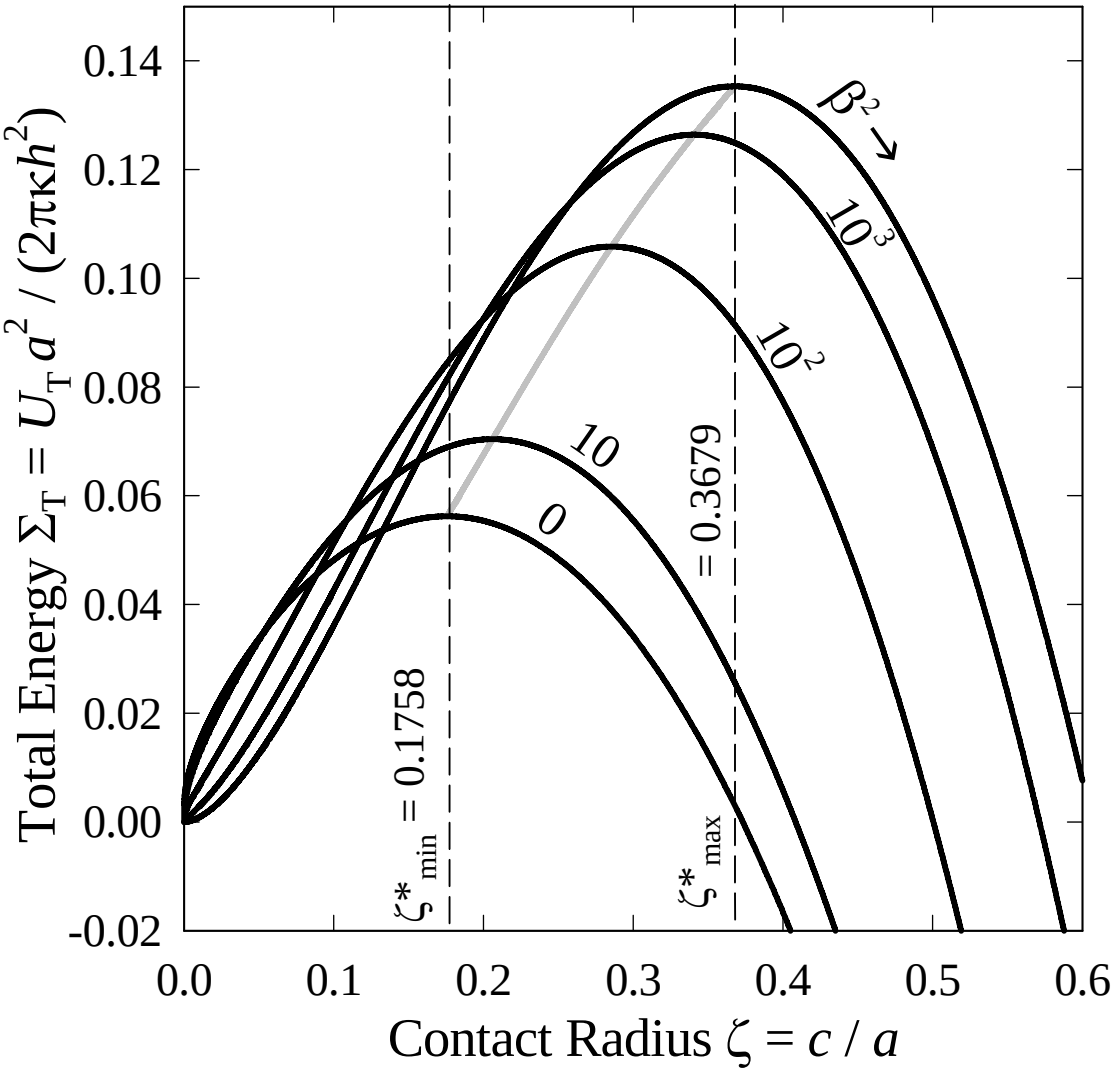

Figure 3.5. System Energy at a Range of Residual Stress with ζ^*_{min} and ζ^*_{max}

Consequently, the "pull-off" shifts to a smaller punch displacement but a larger contact circle. The "pull-off" locus follows a gray curve bounded by $\zeta^*_{min} \le \zeta^* \le \zeta^*_{max}$

with $\zeta^*_{min} = 0.1758$ for $\beta = 0$ and $\zeta^*_{max} = e^{-1} = 0.3679$ for $\beta \rightarrow \infty$. A large residual leads to a stiff film where stretching deformation dominates and bending becomes negligible. Figure 3.6 shows $\zeta^*(\beta^2)$, which is independent of Γ. The open circle on the curve denotes the "pull-off" event at point C in Figure 3.3 with $\Gamma = 1.00$ and $\beta = 1.00$.

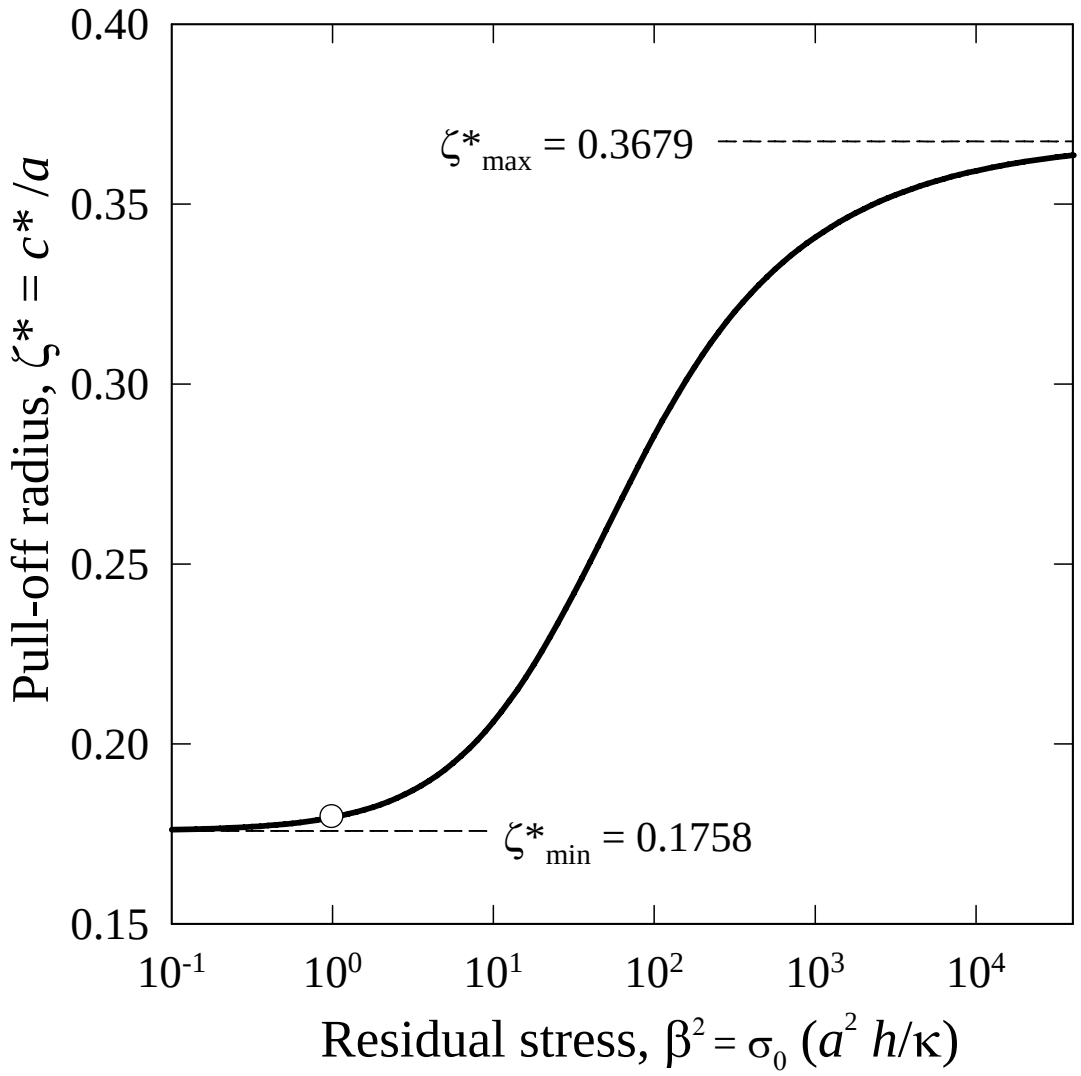

Figure 3.6 Change in "Pull-Off" Radius as a Result of Increase in Tensile Residual Stress

3.4. CONSTITUTIVE RELATION

To derive $\varphi(\omega_0)$ for the delamination process, ζ can be eliminated from (3.7) and (3.12). To circumvent the formidable mathematical operation, the exact form of $\varphi(\omega_0)$ can be found by a parametric method with a varying parameter ζ, because both φ and ω_0 are functions of ζ. Figure 3.7 shows $\varphi(\omega_0)$ with $\Gamma = 1.00$ and $\beta = 1.00$ for a punch with radius $\zeta_A = 0.5702$.

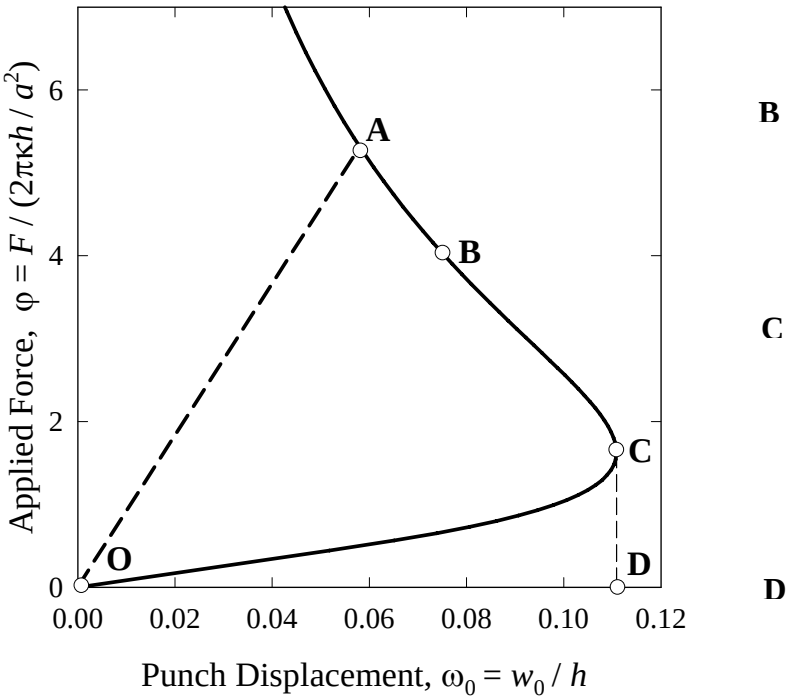

Figure 3.7 Delamination Trajectory of the 2-D Model Constitutive Relation

Delamination follows the trajectory OABCD (c.f. curve ABC in Figure 3.3). Along the path OA, external loading results in a continuous deformation of the annulus (a – c), but does not cause delamination because of insufficient elastic energy stored in the film. According to Equation (3.7), the loading process is linear because of the linear $\varphi(\omega_0)$. As the punch moves beyond point A, delamination starts to propagate according to Equation (3.13). Further increase in ω_0 reduces the external load and shrinks the contact

circle along ABC. Point C denotes the last point on the energy balance curve. Here, the gradient of $\varphi(\omega_0)$ tends to infinity, i.e. $(d\varphi/d\omega_0) \rightarrow \infty$. Further increase in ω_0 violates the energy balance. "Pull-off" occurs and the external load drops to zero at D. The critical values of φ^*, ω_0^*, and ζ^* at "pull-off" can be experimentally measured, yielding both the adhesion energy and residual stress. The nonphysical branch CO is a direct result of only mathematical balance of the energy equation and is shown as the dashed curve in Figure 3.3. If the cylinder has exactly the same diameter as the clamped film, then the overhanging annulus ($a - c$) vanishes and a theoretically infinite external load is required to initiate delamination. Such a force singularity is a direct consequence of the *membrane* deformation assumption. When the delaminated annulus has a width much smaller than the film thickness (i.e., $(a - c) << h$) in the crack initiation stage, the mechanical stress is confined to a small region around the delamination front, the characteristics of being a film subjected to bending-stretching is lost, and Equation (1) breaks down. In fact, the initiation load is *finite* in an ultra-thin membrane with zero flexural rigidity [18]. The exact solution for the delamination initiation stage is beyond the scope of this thesis.

The coupling effects of adhesion and residual stress are illustrated in Figures 3.8 and 3.9. Figure 3.8 shows the delamination path with $\beta = 1.00$ with a varying Γ. The curve labeled ABC is identical to that in Figure 3.3. The gray curve connects the "pull-off" events, thus increasing adhesion energy shifts φ^* and ω_0^* to higher values as expected. Because both φ and ω_0 are proportional to $\Gamma^{1/2}$ and ζ^* is a constant for fixed β (c.f. Equations 3.7 and 3.13), it can be easily deduced that $\varphi^* \propto \omega_0^*$. Figure 3.9 shows the delamination path with $\Gamma = 1.00$ with a varying β. The gray curve connects all the "pull-off" events. The limiting case of $\beta \rightarrow \infty$ leads to a remarkable result, namely

$$\varphi^* = \left(\frac{4}{e^2}\right)\frac{1}{\omega_0^*} \tag{11}$$

as derived from (3) and (6), and $\zeta^* = \zeta^*_{\max} = e^{-1}$. Increasing the residual stress stiffens the film and shifts the "pull-off" event to a higher φ^* but a lower ω_0^*.

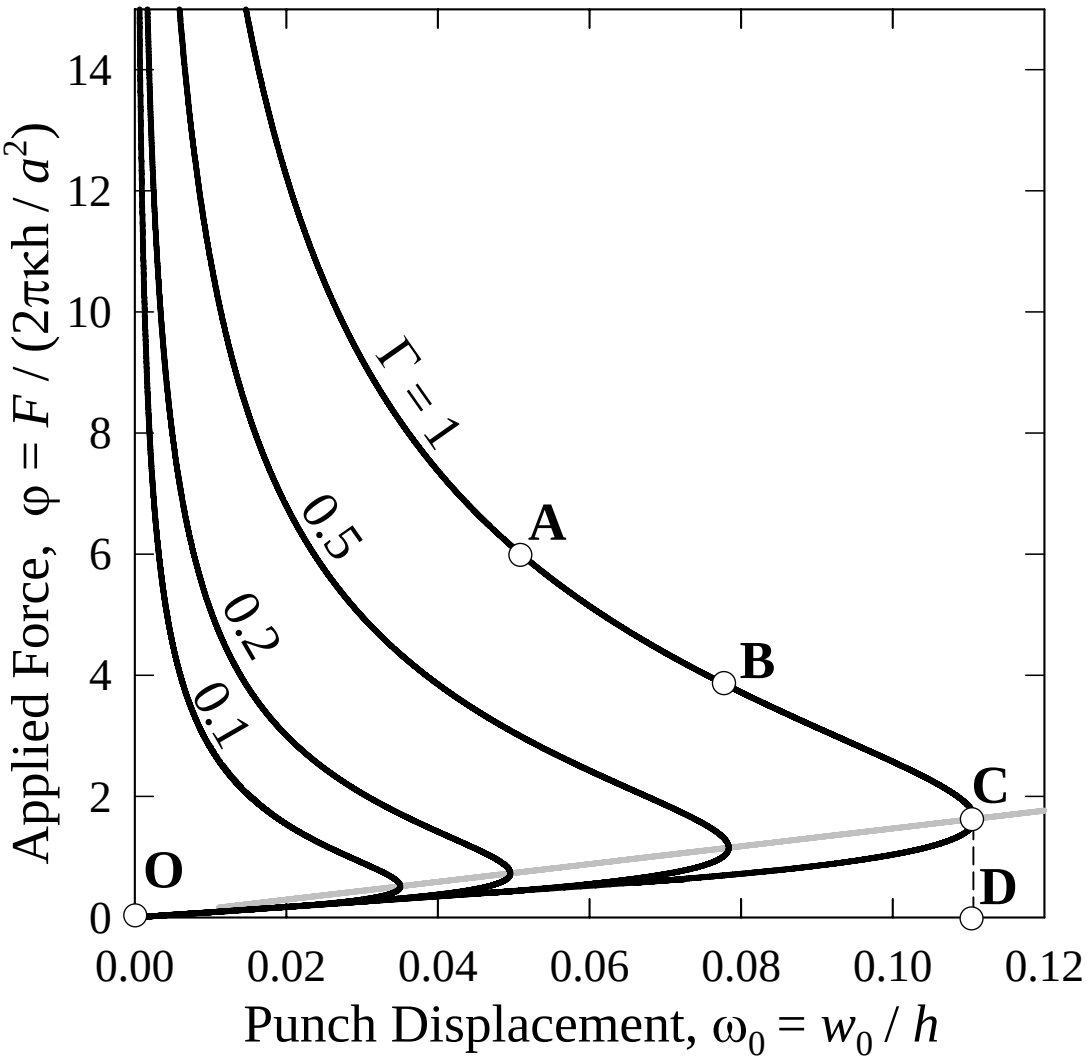

Figure 3.8. Delamination Trajectory under the Effect of Increasing Adhesion Energy

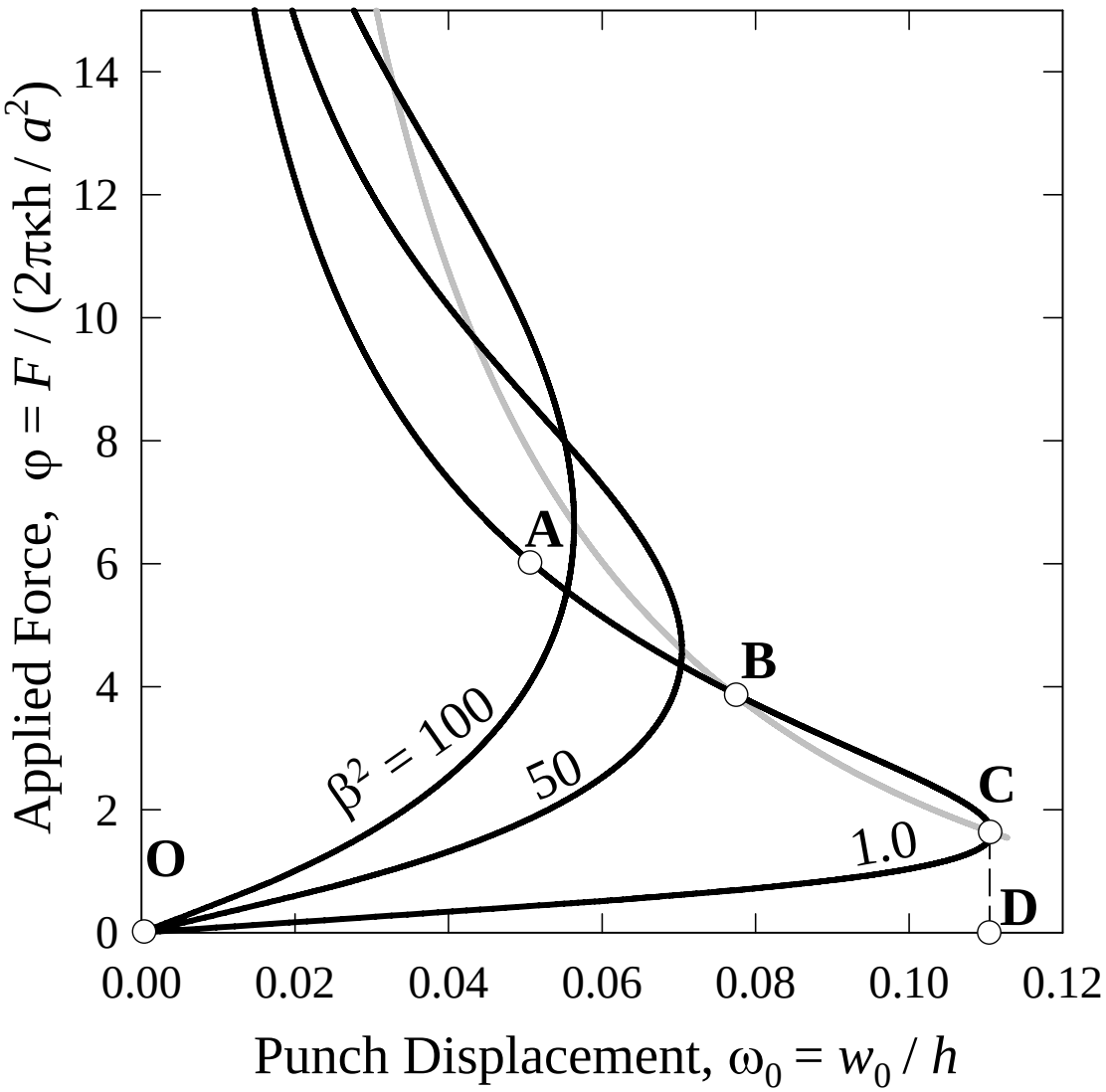

Figure 3.9. Delamination Trajectory under the Effect of Increasing of Tensile Residual

4. DISCUSSION

4.1. GENERAL DISCUSSION OF THE TWO MODELS

A few general remarks regarding the assumptions and implications of the 1-D and 2-D models are warranted. Foremost, the deformed film profile upon external load could lead to a non-zero concomitant membrane stress in addition to the intrinsic residual stress. There are, however, several shortcomings in ignoring σ_m. The error will be most significant at the bending-stretching transition when the total elastic energy U_E comprises comparable bending and stretching components. This occurs when the punch displacement is roughly the film thickness ($w_0 \approx h$) : (i) When the residual stress falls roughly below $\beta_{min} = 1$, the film is governed by bending only and the effect of residual stress can be ignored; (ii) When the residual roughly exceeds $\beta_{max} = 10^3$, the bending component can be ignored; (iii) In the intermediate range ($\beta_{min} < \beta < \beta_{max}$), the concomitant stress should be considered, though its inclusion leads to a slight shift in the mechanical response only. In addition, it is interesting to compare the 1-D model presented here with the 2-D circular film counterpart. The 2-D model predicts a “pull-off” event that leads to a non-zero contact circle prior to a spontaneous delamination. The critical “pull-off” radius was theoretically found and experimentally verified earlier to fall between 0.1757 (for $\beta \rightarrow 0$) and 0.3679 (for $\beta \rightarrow \infty$) of the film radius [17, 18, 20]. It is interesting to compare the 1-D model presented here with the 2-D circular film counterpart. The 2-D model predicts a “pull-off” event that leads to a non-zero contact circle prior to a spontaneous delamination. The critical “pull-off” radius was theoretically found and experimentally verified earlier to fall between 0.1757 (for $\beta \rightarrow 0$) and 0.3679 (for $\beta \rightarrow \infty$) of the film radius [17, 18, 20]. The 1-D model, on the other hand, predicts a “pinch-off” with the contact area gradually and stably shrinking to zero under the fixed-grips configuration. It is logical to deduce that for an elliptical film (intermediate geometry between a circle and a straight line), the critical “pull-off” contact area is expected to be finite and lies between the two extremes. The present work will serve as the asymptotes for an elliptical film-punch system.

Although the main focus of this thesis is in thin film delamination, the complementary adhesion mechanics are virtually equivalent with some remarkable

differences. If a micro-probe is made of a clamped freestanding film to measure the surface forces of a certain sample, then the thermodynamic energy balance can be formulated in exactly the same manner as above, though the zero-range surface force assumed in the current model must be modified accordingly. When the probe moves to a distance w_0^* from the sample surface, the film is energetically more favorable to jump into adhesive contact, or "pull-in". In fact, "pull-off" and "pull-in" are equivalent in thermodynamic terms. However, a long-range interaction is required for "pull-in" to occur. If the surface force range is shorter than w_0^*, then the film will stay largely undeformed because of an energy barrier across the gap. Conversely, a long-range force with range exceeding w_0^* will trigger "pull-in."

4.2. APPLICATION TO A 1-D MEMS-RF SWITCH

The rectangular model can be applied to MEMS-RF switch and is taken as an example to illustrate the usage of the new model (Figure 2.1). The device has a gap of fixed separation, w_0, between the bridge and the electrostatic pad underneath. Unlike the moveable punch in this new model, the pad is at rest and fixed in position. Adhesion occurs when an electrostatic attraction compels the bridge to make contact with the substrate. Upon grounding the pad, the bridge-pad dielectric space is free of long-range surface forces, but the adhesive interface is supported by short-range attractions such as van der Waals interaction and water meniscus due to relative humidity in the environment [27]. Thus, the total energy of the system thus becomes $U_T = U_E + U_S$, because $U_P = 0$. For a linear mechanical response $\varphi(\omega_0)$ (c.f. Equation (2.5)), $U_E = -(\frac{1}{2})Fw_0$. The resulting U_T, the energy balance, and the delamination mechanics are therefore identical to what was derived above, consistent with the principle of equivalence of fixed load and fixed grips in linear systems [25]. There are several significant implications in the switch design. Should the bridge-pad gap be designed such that $\omega_0 < \omega_0^*$, removal of the electrostatic potential does not detach the bridge but leaves it in adhesive contact with the pad with a contact length given by (2.11). For $0 < \omega_0 < \omega_0^*$, a non-zero contact length is expected as shown in Figure 2.3 by A, B, and C. At D, the contact is reduced to a central line ($\lambda = 0$). The device is operational only when the gap exceeds a minimal value of $\omega_0^* = (\omega_0)_D$ given by (2.17). Stronger adhesion requires a

larger gap, and stiffer film with a larger residual stress requires a smaller gap. The critical value of ω_0^* is also related to the materials properties of the bridge of specific span and width. Another outcome of the present model is the mechanical force acting on membrane by the substrate (or punch), which can be found by substituting Equation (2.17) into (2.12). If the resulting bending moments exceed the yielding limit of the bridge materials, plastic deformation occurs and the device fails [28]. The coupled effect of adhesion and residual stress must be considered in order to design the optimal geometry of a MEMS-RF switch.

The present model is compared to an existing model in the literature. Yang [29] derived an elastic model similar to MEMS-RF switch for bending deformation only but predicted a fixed "jump-in" area with $\lambda = ¼$, contrasting the variable "pull-off" λ^* derived here that depends on the coupled adhesion energy and residual stress. A possible discrepancy is Yang's assumption of $U_T = U_E + U_S = 0$, which is based on a reversible energy balance and zero energy dissipation. The criterion virtually implies that all elastic energy is converted into surface energy when the adhesive contact is made. However, every incremental growth of the delamination front requires the overhanging non-contact part of the bridge to remain under elastic strain with $dU_E \neq 0$. To establish a proper energy balance, the elastic energy in the pre- and post-delamination states must be considered. In other words, $U_T \neq 0$ but only $dU_T = 0$ at equilibrium. The constant "jump-in" contact area so derived is therefore doubtful. In fact, the nomenclature "jump-in" seems to be inappropriate. Yang's model is based on a zero-range surface force that causes adhesion. For a grounded electrostatic pad, there exists no long-range force to trigger "jump-in" occurs, though the energy state of an adhered bridge is lower than that of a free bridge. In the literature, "pull-in" is always referred to as the bridge being forced into contact with the pad by the applied electrostatic potential, regardless of interfacial adhesion. "Pull-in" occurs in an ideal MEMS-RF switch even when the adhesion energy is zero. In another paper for a circular membrane clamped at the perimeter [30], the author adopted a uniform pressure to represent the external load on the film, instead of a Dirac delta function as in (3.1). Such approximation is believed to lead to erroneous results because (i) mechanical load on the membrane within the contact circle must vanish to ensure a planar contact circle with $dw/dx = 0$, and (ii) the load without the

contact edge must also vanish because the overhanging annulus is obviously not subject to any external forces.

4.3. APPLICATION TO THE BIOLOGICAL ADHESION-DELAMINATION PROBLEM

Cell locomotion is a relevant example of the 2-D axisymmetric in biology. When a cell attempts to move in a certain direction, the actin filaments construct a makeshift pseudopodium that makes an adhesive contact or focal adhesion plaque with the substrate, similar to Figure 3.1. Retraction of the hind “leg” then pulls the anchoring membrane out of contact, allowing the cell to move a step forward. The construction and destruction of the adhesive contacts can be discussed using the 2-D model. If the intersurface forces are ligand-receptor interaction in origin, then the adhesion mechanism also involves receptor diffusion in and out of the interface, as discussed in detail by Freund and Lin [31] using a model similar to the present work. Freund [31] assumes plate-bending of the cell wall in formation of focal adhesion plaque and ignores all membrane stretching, which could be the main deformation mode in many ultra-thin biological membranes. Residual membrane stress generated a result of osmosis in the case of differential gradients of liquid concentration within and without the cell [3]. Also, viscoelasticity of the cell membrane and network of actin filaments and extra-cellular matrix further complicates the locomotion mechanics [32]. The simple model here is not meant to be comprehensive in explaining these complex biological phenomena, but to provide a rigorous solid-mechanics basis for the underlying mechanical aspects. Correlation between mechanics and biochemistry is beyond the scope of this thesis.

5. CONCLUSION

Rigorous theoretical models are constructed for the delamination mechanics of a pre-stressed rectangular film and circular film adhered to a rigid punch based on a thermodynamic energy balance. The models provide the engineering performance equation [33], which relate to the following factors: (i) the structural index of thin film delamination, as well as mixed plate-bending and tensile residual stress; (ii) the measurable quantities of applied load, punch displacement (and the equivalent bridge-pad gap) and contact area; (iii) the geometrical factor of film thickness and length span, and (iv) the materials parameters of the elastic modulus and Poisson's ratio of the film, adhesion energy at the film-substrate interface, and residual membrane stress. For the 2-D axisymmetric model, "pull-off" reminiscent of the JKR model and the associated force-displacement relation are derived and quantified in terms of the aforementioned quantities. The model is essential in investigating many adhesion-delamination phenomena involving thin films from micro- to macro-scale. The trends and graphs have significant impacts on the design and fabrication of some MEMS involving moveable thin film components, as well as cell adhesion and locomotion.

APPENDIX A

M. F. WONG, G. DUAN, AND K.-T. WAN
JOURNAL OF APPLIED PHYSICS 101, 024903 (2007)

APPENDIX B

M. F. WONG, G. DUAN, AND K.-T. WAN
THE JOURNAL OF ADHESION, 83:67–83, 2007

APPENDIX C

MECHANICS OF FILM-FILM DELAMINATION OF FLEXIBLE MEMBRANE

Presentation at

THE ADHESION SOCIETY 30TH ANNUAL MEETING, 2007, TAMPA FL

(Feb 21st 2007)

APPENDIX D

B. F. JU, K. K. LIU, M. F. WONG AND K.-T. WAN
Engineering Fracture Mechanics 74, (2007) 1101-1106

BIBLIOGRAPHY

[1] S. Huebner, B.J.B., R. Grimm and G. Cevc, *Lipid-DNA Complex Formation: Reorganization and Rupture of Lipid Vesicles in the Presence of DNA As Observed by Cryoelectron Microscopy*. Biophysical Journal, 1999. **76**: p. 3158-3166.

[2] Alberts, B., Bray, D., Lewis, J., Raff, M., Roberts, K., and Watson, J.D., *Molecular Biology of The Cell*. 1994, New York: Garland.

[3] Wan, K.-T. and Liu, K.K., *Contact mechanics of a thin walled capsule adhered onto a rigid planar substrate.* Medical and Biological Engineering and Computing, 2001. **39**: p. 605-608.

[4] Liu, K.K., Wang, H.G., Wan, K.-T., Liu, T., and Zhang, Z., *Characterizing capsule-substrate adhesion in presence of osmosis.* Colloids and Surfaces B: Biointerfaces, 2002. **25**(4): p. 293-298.

[5] Foo, J.J., Chan, V., and Liu, K.K., *Contact deformation of liposome in the presence of osmosis.* Annals of Biomedical Engineering, 2003. **31**: p. 1279-1286.

[6] Foo, J.J., Liu, K.K., and Chan, V., *Viscous drag of deformed vesicles in an optical trap: numerical simulation and experiments.* AICHE, 2004. **50**(1): p. 249-254.

[7] Israelachvili, J.N., *Intermolecular and Surface Forces*. 2nd Edition ed. 1991, London: Academic Press.

[8] Knapp, J.A. and DeBoer, M.P., *Mechanics of microcantilever beams subject to combined electrostatic and adhesive forces.* Journal of Microelectromechanical Systems, 2002. **11**: p. 754-764.

[9] Wu, D., Fang, N., Sun, C., and Zhang, X., *Stiction problems in releasing of 3D microstructures and its solution.* Sensors and Actuators A: Physical, 2006. **128**: p. 109-115.

[10] Wang, C.M., Zhang, Y.Y., Ramesh, S.S., and Kitipornchai, S, *Buckling analysis of micro- and nano-rods/tubes based on nonlocal Timoshenko beam theory.* Journal of Physics, 2006. **39**: p. 5.

[11] Withers, J.R. and Aston, D.E., *Nanomechanical measurements with AFM in the elastic limit.* Advances in Colloid and Interface Science, 2006. **120**: p. 57-67.

[12] Begley, M.R., *The impact of materials selection and geometry on multi-functional bilayer micro-sensors and actuators.* Journal of Micromechanics and Microengineering, 2005. **15**: p. 2379-2388.

[13] Najar, F., Choura, S., El-Borgi, S., Adbdel-Rahman, E., and Nayfeh, A., *Modeling and design of variable-geometry electrostatic microactuators.* Journal of Micromechanics and Microengineering, 2005. **15**: p. 419-429.

[14] Kendall, K., *Molecular Adhesion and Its Application: The Sticky Universe*. 2001, New York: Kluwer Academic / Plenum Publishers.

[15] Maugis, D., *Contact, Adhesion and Rupture of Elastic Solids*. 2000, New York: Springer.

[16] Wan, K.-T., *Adherence of an axisymmetric flat punch onto a clamped circular plate - Transition from a rigid plate to a flexible membrane.* Journal of Applied Mechanics, 2002. **69**: p. 110-116.

[17] Wan, K.-T. and Dillard, D.A., *Adhesion of a flat punch adhered to a thin pre-stressed membrane.* Journal of Adhesion, 2003. **79**: p. 123-140.

[18] Raegen, A.N., Dalnoki-Veress, K., Wan, K.-T., and Jones, R.A.L., *Measurement of adhesion energies and Young's modulus in thin polymer films using a novel axi-symmetric peel test geometry.* The European Physical Journal E, 2006. **19**: p. 453-459.

[19] Wan, K.-T. and Kogut, L., *The coupling effect of interfacial adhesion and tensile residual stress on a thin membrane adhered to a flat punch.* Journal of Micromechanics and Microengineering, 2005. **15**: p. 778-784.

[20] Wan, K.-T., *Adherence of an axial symmetric flat punch on a flexible membrane.* Journal of Adhesion, 2001. **75**(4): p. 369-380.

[21] Wan, K.-T. and Duan, J., *Adherence of a rectangular flat punch onto a clamped plate - Transition from a rigid plate to a flexible membrane.* Journal of Applied Mechanics, 2002. **69**: p. 104-109.

[22] Wan, K.-T., Guo, S., and Dillard, D.A., *A theoretical and numerical study of a thin clamped circular film under an external load in the presence of residual stress.* Thin Solid Films, 2003. **425**: p. 150-162.

[23] Parker, A.P., *The mechanics of fracture and fatigue: An introduction* 1981: E. & F.N. Spon.

[24] Timoshenko, S.P. and Woinowsky-Krieger, S., *Theory of Plates and Shells*. 2 ed. 1959, New York: McGraw-Hill.

[25] Lawn, B.R., *Fracture of brittle solids*. Cambridge solid state science series, ed. Davis, E.A. and Ward, I.M. 1993, Cambridge, UK: Cambridge University Press.

[26] Agca, Y., Liu, J., McGrath, J., Peter, A., Critser, E., and Critser, J., *Membrane permeability characteristics of Metaphase II mouse oocytes at various temperatures in the presence of Me2 SO.* Cryobiology, 1998. **36**: p. 287-300.

[27] Mastrangelo, C.H. and Hsu, C.H., *Mechanical stability and adhesion of microstructures under capillary forces - Part II: Experiments.* Journal of Microelectromechanical Systems, 1993. **2**(1): p. 44-55.

[28] Nicola, L., Xiang, Y., Vlassak, J.J., E.Van_der_Giessen, and Needleman, A., *Plastic deformation of freestanding thin films: experiments and modeling.* Journal fo the Mechanics and Physics of Solids, 2006. **54**: p. 2089-2110.

[29] Yang, F., *Contact deformation of a micromechanical structure.* Journal of Micromechanics and Microengineering, 2004. **14**: p. 263-268.

[30] Yang, F., *Adhesive contact of axisymmetric suspended miniature structure.* Sensors and Actuators A, 2003. **104**: p. 44-52.

[31] Freund, L.B. and Lin, Y., *The role of binder mobility in spontaneous adhesive contact and implications for cell adhesion.* Journal of the mechanics and physics of solids, 2004. **52**: p. 2455-2472.

[32] Boal, D., *Mechanics of the cells*. 2002, New York: Cambridge University Press.

[33] Ashby, M.F., *Materials selection in mechanical design*. 3rd Edition ed. 2005, Woburn, MA: Butterworth-Heinemann.

VITA

Ming Fung Wong was born on April 19th 1983 in Hong Kong as the first child of Mr. Wing-fai Wong and Mrs. Chung-siu Lau. He first entered the United States as a High School Exchange Student in 2000. His host family was Mr. Cleve and Mrs. Joan Reyes in Piedmont, Missouri. Wong spent the exchange year in Clearwater R-1 High School and obtained his high school diploma in 2001.

Wong attended the University of Missouri – Rolla from 2001 to 2005 and earned a Bachelor of Science degree in Mechanical Engineering with a minor in Aerospace Engineering. Wong's research in film thin adhesion-delamination was supported by the OURE (Opportunity of Undergraduate Research Experience) Program in 2004 under the advice of Dr. Kai Tak Wan. The original research model was extended to a range of technical areas including film adhesion and micro-electo mechanical system. During the years in University of Missouri – Rolla, Wong was a student member of Formula SAE, the American Society of Mechanical Engineers (ASME) and the International Society for Optical Engineering (SPIE). He earned his Master of Science Mechanical Engineering degree in August 2007.